THE JOURNAL OF BIOLOGICAL CHEMISTRY
Vol. 256, No. 3, Issue of February 10, pp. 1432-1446, 1981
Printed in U.S.A.

Nuclear Magnetic Resonance of Heme Protein Crystals

GENERAL ASPECTS*

(Received for publication, July 29, 1980, and in revised form, September 18, 1980)

T. Michael Rothgeb‡ and Eric Oldfield§

From the School of Chemical Sciences, University of Illinois at Urbana-Champaign, Urbana, Illinois 61801

A new technique capable of determining the static and dynamic structures of heme protein crystals is reported. It is shown that microcrystals of a variety of paramagnetic heme proteins, suspended in ~90% saturated $(NH_4)_2SO_4$, may be perfectly aligned by an intense static external magnetic field, H_0, due to the large anisotropy in the magnetic susceptibility of the protein caused by the paramagnetic center. Myoglobin from sperm whale (*Physeter catodon*) was isotopically enriched at the C^ϵ methyl groups of methionine residues 55 and 131 with either ^{13}C or ^2H and studied in the crystalline solid state by ^2H-quadrupole echo and ^{13}C-Fourier transform nuclear magnetic resonance spectroscopy. It was found that suspensions of both high ($S = 5/2$) and low ($S = 1/2$) spin ferric forms of the labeled protein were ordered, the axis of ordering being approximately perpendicular to the low temperature minimum g tensor valve, even though upper Kramers levels are populated at room temperature. The paramagnetic Co^{II} derivative "coboglobin" showed similar ordering behavior, but the diamagnetic carboxymyoglobin was unaffected. The magnetic ordering method permits the recording of "single crystal" NMR spectra from microcrystalline arrays of proteins which cannot be prepared in large enough form (~1 cm^3) for single crystal NMR spectroscopy and thereby allows the resolution and assignment of numerous single atom sites in the crystalline solid state. The information from a "single crystal" NMR spectrum combined with that obtained on the crystal powder allows for the direct determination of (i) the spatial orientation of the particular labeled residue within the protein crystal and (ii) the rates and types of side chain motion. Resonances were assigned by spin label broadening experiments and by use of existing x-ray data to predict ^2H-NMR spectra. This new technique opens up the possibility of determining directly the dynamic structure of protein crystals and of comparing the structures of proteins in the crystalline solid state with that in solution and is applicable to other heme proteins, *e.g.* catalase.

Over the past twenty years, there have been an impressive number of studies of the structure of proteins, both in the crystalline solid state (1) and in solution (2, 3). Direct information about protein structure comes from x-ray crystallography of solid samples, while solution structural information has been obtained by nuclear magnetic resonance spectroscopy. Of the two methods, x-ray diffraction gives the most direct three-dimensional or spatial structural information, while NMR spectroscopy is more suited to determination of the dynamical aspects of protein structure (4, 5). Unfortunately, however, it is not yet possible to use diffraction methods to obtain detailed spatial (or dynamical) structural information about proteins in solution, so questions about differences between solution and crystal structure appear insoluble by any direct method, although such questions do seem to have been answered indirectly to the satisfaction of many workers (6, 7).

In principle, however, nuclear magnetic resonance spectroscopy might be used to answer the question, "Is the structure of a protein the same in solution as it is in a crystal?" by using a combination of techniques to obtain high resolution solid state spectra. While it has recently been shown to be feasible (8) to obtain high resolution ^{13}C-NMR spectra of randomly oriented protein crystal powders using "magic angle" spinning methods (8-10) it is not yet possible to interpret the results in a quantitative manner. Since it is unlikely that there will be any rapid solution to the problem of interpreting ^{13}C-chemical shifts of proteins in structural terms, we have developed a new NMR technique capable of giving directly static and dynamic structural information about proteins in condensed phases, such as crystals and membranes. Our initial efforts discussed in this publication are directed at "calibrating" our method by showing that NMR may be used to directly determine methionine methyl group orientation in crystals of sperm whale (*Physeter catodon*) myoglobin, the first protein whose structure was determined by x-ray (11) and neutron diffraction (12). While heme group orientations in proteins have been investigated previously by optical (13) and electron spin resonance techniques (14), these methods are relatively indirect. While it is doubtful that any method capable solely of confirming the correctness of existing x-ray structures would have any utility, we indicate how our method may be used (i) to determine in protein crystals too small to be studied by x-ray crystallography the orientation of various residues, (ii) to determine in a direct fashion the rates and types of motion and activation energies for motion of various residues in protein crystals, which is presumably one of the main reasons for differences between the activities of enzymes and other proteins in solution and in the crystalline solid state (15), and (iii) to determine, in principle, differences between solution and crystal structure by comparison of chemical shifts in the two states. Moreover, we note that our technique may be used to determine static and dynamic structures of membrane

* This work was supported by the National Institutes of Health (Grant HL-19481), by equipment grants provided by the National Science Foundation (Grants PCM 78-23021, PCM 79-23170) and the Alfred P. Sloan Foundation, by the Los Alamos Scientific Laboratory Stable Isotope Resource, which is jointly supported by the United States Department of Energy and the National Institutes of Health (Grant RR-99962), and by the University of Illinois National Science Foundation Regional Instrumentation Facility (Grant CHE 79-16100). The costs of publication of this article were defrayed in part by the payment of page charges. This article must therefore be hereby marked "*advertisement*" in accordance with 18 U.S.C. Section 1734 solely to indicate this fact.

‡ National Science Foundation Postdoctoral Fellow.

§ Alfred P. Sloan Research Fellow, 1978-1980; United States Public Health Service Research Career Development Awardee, 1979-1984 (Grant CA-00595).

proteins, including the details of protein-lipid interactions.[1]

Most of the above questions could be answered if it were possible to obtain and interpret high resolution NMR spectra of single protein crystals. For studies at natural abundance, only carbon-13 NMR appears to be promising from the standpoint of protein-crystal studies (8). Carbon-13 has a spin $I = 1/2$ and a 1.1% natural abundance, and current instrumentation sensitivity is probably adequate to observe resolved single carbon atom resonances in small (M_r ~20,000) proteins if ~1 cm^3 crystals can be grown (8). This is a difficult task. Protons, which have a spin $I = 1/2$ and 100% natural abundance, are highly sensitive, but proton NMR would seem to be inappropriate because of the large dipolar broadenings seen between protons in the solid state, which can only be partially removed by application of complex pulse sequences (16). Similarly, natural abundance studies with the quadrupolar nuclei deuterium (^2H, $I = 1$, 0.015% natural abundance) and oxygen-17 (^{17}O, $I = 5/2$, 0.037% natural abundance) and with the spin $I = 1/2$, 0.37% abundant nucleus nitrogen-15 are not presently feasible at the natural abundance level. Finally, studies with the quadrupolar species nitrogen-14 (^{14}N, $I = 1$, 99.63% abundance) seem technically feasible (17), but there would seem to be substantial difficulties in making assignments in a protein crystal and of resolving individual atomic sites in solution spectra.

Since it seems unlikely that sufficiently large single crystals can be grown for most of the above experiments, new strategies must clearly be developed in order to obtain information about protein crystal static and dynamic structure using NMR spectroscopy. The initial step, where possible, will be to selectively enrich with the nucleus of interest, a strategy likely to prove useful for ^2H, ^{13}C, ^{15}N, and ^{17}O. With more effort, "inverse" labeling of ^1H in a ^2H matrix or ^{14}N in an ^{15}N matrix, may be utilized. Still, however, there remains the problem of growing rather sizeable single crystals.

Fortunately, however, we have now developed methods (18) which permit observation of resolved resonances from individual sites in protein crystals by means of externally applied ordering fields on protein microcrystals. We show in this publication that it is now possible to resolve, assign, and determine the spatial organization of a variety of groups in sperm whale (*P. catodon*) myoglobin microcrystals, observations which open up the possibility of determining directly the dynamics of motion of residues in protein crystals, a topic of considerable current interest (19, 20), as well as providing the beginnings toward a resolution of the crystal/solution structure question. In addition, our general methods are applicable to membrane protein structure determinations.[2]

EXPERIMENTAL PROCEDURES

Theoretical Background

NMR Spectroscopy—As discussed above, it is particularly difficult to grow protein crystals of sufficient size to permit single crystal NMR studies, since typically 1 g or more of material would be required for a natural abundance NMR investigation (8, 21–24). Even with, for example, ^2H or ^{13}C labeling, large well formed single crystals of ~20 mm^3 volume will generally be required. We have, therefore, approached the problem from a rather different viewpoint.

Let us first consider just what it is that differentiates a "solution" from a "crystal" spectrum, both for ^{13}C and ^2H nuclei, the most promising candidates for protein-crystal NMR probes.

Quite generally, we can write for a nucleus a Hamiltonian

$$\mathcal{H} = \mathcal{H}_Z + \mathcal{H}_Q + \mathcal{H}_{DD} + \mathcal{H}_{CSA} + \mathcal{H}_{SC} \quad (1)$$

where $\mathcal{H}_Z$, $\mathcal{H}_Q$, $\mathcal{H}_{DD}$, $\mathcal{H}_{CSA}$, and $\mathcal{H}_{SC}$ represent the Zeeman, quadrupole, dipole-dipole, chemical shift, and scalar coupling interactions, respectively. Now for ^2H ($I = 1$) $\mathcal{H}_{DD}$, $\mathcal{H}_{CSA}$, and $\mathcal{H}_{SC}$ are small; thus we may write

$$\mathcal{H} = \mathcal{H}_Z + \mathcal{H}_Q \quad (2)$$

or more explicitly

$$\mathcal{H} = -\gamma_n \hbar H_0 I_{z'} + \frac{e^2qQ}{4I(2I-1)}(3I_z^2 - I^2) \quad (3)$$

where the symbols have their usual meanings (25), the solutions for the energies being

$$E_m = -\gamma_n \hbar H_0 m + \frac{e^2qQ}{4}\frac{3\cos^2\theta - 1}{2}(3m^2 - 2) \quad (4)$$

the allowed transitions corresponding to $+1 \leftrightarrow 0$ and $0 \leftrightarrow -1$ giving rise to a "quadrupole splitting" of the absorption line with separation between peak maxima of

$$\Delta\nu = \frac{3}{2}\frac{e^2qQ}{h}\frac{3\cos^2\theta - 1}{2} \quad (5)$$

where θ is the angle between the magnetic field H_0 and the principal axis of the electric field gradient tensor (frequently the C—D bond vector).

For rigid polycrystalline solids all values of θ are possible and one obtains a so-called "powder pattern," Fig. 1*A* having a peak separation corresponding to $\theta = 90°$, for which $\Delta\nu = 3e^2qQ/4h$, and a shoulder separation corresponding to $\theta = 0°$, that is $\Delta\nu = 3e^2qQ/2h$. It is Equation 5 or a slightly modified version of it taking into account motion of the group under consideration (*e.g.* a methyl group spinning about its C_3 axis) that permits us to obtain information about protein crystal structure. For example, if a heme group labeled as ^2H at its α, β, γ, and δ meso-positions were oriented in such a way in a crystal that the plane of the heme ring was at 90° to the external magnetic field H_0, then a "sharp line" spectrum (Fig. 1*B*) having $\Delta\nu_Q$[3] ~138 kHz would be obtained, *i.e.* the splitting would be three-quarters of the quadrupole coupling constant, which is ~184 kHz for aromatic systems (26).

For carbon-13 (spin $I = 1/2$) nuclei, there is no quadrupole interaction, and under conditions of strong proton irradiation the Hamiltonian in most cases will be

$$\mathcal{H} = \mathcal{H}_Z + \mathcal{H}_{CSA} \quad (6)$$

Without elaborating further, we note that the energies corresponding to the transition $+1/2 \leftrightarrow -1/2$ will in general give rise to a powder pattern lineshape having $\sigma_{11} \neq \sigma_{22} \neq \sigma_{33}$ as illustrated in Fig. 1*C* (16). In the presence of rapid axial motion (*i.e.* for motions occurring on a timescale fast compared to $|\sigma_{33} - \sigma_{11}|$ expressed in frequency units) then an axially symmetric powder pattern having a shape identical with that of one of the transitions shown in Fig. 1*A* will be observed (Fig. 1*D*). The sign of the anisotropy depends on the chemical nature of the group and the motion(s) involved.

It should, therefore, be possible to determine the orientation of a particular ^2H-labeled group in an ordered system from its quadrupole splitting ($\Delta\nu_Q$) and knowledge of the breadth of the powder pattern distribution. This in turn should permit calculation of its ^{13}C-chemical shift. Since averaging of the chemical shift interactions in solution leads to an isotropic spectrum having

$$\sigma_i = \frac{1}{3}\mathrm{Tr}\sigma \quad (7)$$

it should, therefore, be possible to obtain from crystal spectra chemical shifts which may be compared with solution chemical shifts to begin to assess any differences in structures between the two states. More importantly, however, success in obtaining ^2H- or ^{13}C-NMR spectra from ordered solids will permit resolution of numerous sites and will thereby enable determination of their dynamics to be determined, in addition to average orientation.

Note that in solution, both the second rank tensor interactions

[1] E. Oldfield and R. Kinsey, data to be published.

[2] E. Oldfield and R. Kinsey, unpublished results.

[3] The abbreviations used are: $\Delta\nu_Q$, quadrupole splitting; TEMPAMINE, 4-amino-2,2,6,6-tetramethyl-piperidinooxyl; Mb, myoglobin; CoMb, cobalt derivative of myoglobin "coboglobin"; MbH_2O, high spin aquoferrimyoglobin; MbCN, low spin cyanoferrimyoglobin; δ, half-width at half-height of a Lorentzian broadening function; Me, methyl.

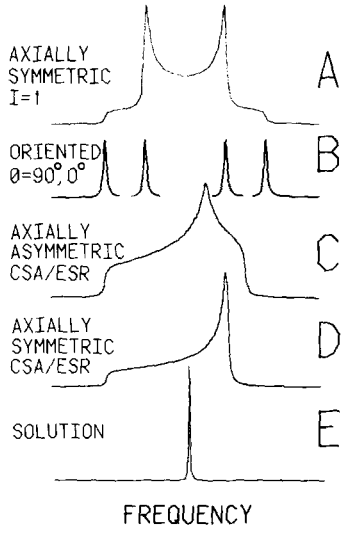

FIG. 1. **Computer-simulated experimental lineshapes expected for deuterium NMR, carbon-13 NMR, and ESR spectroscopy.** *A*, axially symmetric $I = 1$ lineshape (^{2}H-NMR). *B*, oriented sample ^{2}H-NMR lineshape showing parallel and perpendicular edge absorptions. *C*, axially asymmetric chemical shift anisotropy (*CSA*; carbon-13) or electron spin resonance lineshape. *D*, axially symmetric chemical shift anisotropy (carbon-13) or electron spin resonance lineshape. *E*, solution NMR lineshape.

described above are averaged to zero due to rapid particle tumbling, and conventional "high resolution" ^{2}H and ^{13}C spectra may be obtained (21-24, 27, 28) as shown in Fig. 1*E*.

For electron spin resonance spectra, powder-type distribution spectra similar to those illustrated in Fig. 1, *C* and *D*, are frequently encountered. For the systems discussed in this publication we show that the maximum g tensor component, which corresponds to the ground state maximum magnetic susceptibility component, is as expected aligned along the field direction in the magnetically ordered systems. The results we present, therefore, open up the possibility of obtaining relatively high resolution ESR spectra of microcrystalline metalloenzymes containing several different metal sites.

Criteria for Solid State Spectra—As stated above, it is at present exceedingly difficult to grow sufficiently large crystals of proteins for single crystal NMR studies, although microcrystals of a wide variety of proteins are very simple to prepare (29). Since we are ultimately interested in crystal/solution comparisons, it is important to define at what point NMR spectra will be characteristic of a crystal. What is the minimum size particle which will give "solid" rather than "solution" spectra?

For ^{2}H-NMR, we expect particles having isotropic rotational correlation times (τ) $\gg 10^{-5}$ s to give solid-like spectra, since only motions faster than the quadrupole coupling ($e^2qQ/h \sim 200$ kHz) will be effective in motional narrowing. This corresponds to correlation times in the $\gtrsim 10$ μs range, characteristic of particles of $\gtrsim 200$ Å radius undergoing Brownian motion in water. For ^{13}C, the appropriate timescale for solid-like NMR spectra would be $\gtrsim |\sigma_{11} - \sigma_{33}|^{-1}$ s, corresponding to correlation times close to a millisecond, expected for particles of radius $\gtrsim 1000$ Å, while for solid state electron spin resonance spectra the appropriate timescale is $\sim |g_{zz} - g_{xx}|^{-1}$ s, which varies considerably from one paramagnetic protein to another, but in the case of myoglobins would invariably result in powder-type spectra from even the smallest aggregates. These calculations indicate that solid state NMR and ESR spectra will almost always be obtained from microcrystallites that can be resolved under a light microscope corresponding to particle radii $\gg 5000$ Å. For such particles, contributions to the observed spectra from exposed surface protein molecules will of course be negligible.

Field Ordering Effects—The above considerations indicate that solid state structural information will be obtained from protein microcrystals of $\sim 10^{-2}$ cm dimensions. The problem is, therefore, simply one of aligning the microcrystals. Here, there are at least three possible approaches to obtaining oriented samples: (i) magnetic ordering, (ii) electric ordering, and (iii) mechanical ordering.

For a molecule or particle having a magnetic susceptibility χ, the magnetic energy in a field of intensity H is

$$E = -\tfrac{1}{2} H \cdot \chi \cdot H \tag{8}$$

while for a similar particle having a dipole moment μ in an electric field of intensity F the energy is

$$E = -\mu \cdot F \tag{9}$$

Back of the envelope calculations using typical protein dipole moments (30) of say 400 Debyes and magnetic susceptibilities (χ) corresponding to ESR g values of say $g_{max} = 3$, $g_{min} = 1$, led us to believe that for even the smallest protein microcrystals ($\sim 10^{-3}$ cm dimensions) that it should be possible to make both the electric and magnetic interaction energies considerably in excess of the thermal energy kT (per particle), in which case it should be possible to obtain highly ordered samples. Theoretically and experimentally, the situation is more complex, however.

The magnetic energy in our high spin ferric heme crystals may be written quite generally as

$$E = E_{min} \cos^2 \theta + E_{max} \sin^2 \theta \tag{10}$$

where E_{max} and E_{min} are the maximum and minimum potential energies of the particle in the magnetic field, and θ is the angle between the axis of maximum susceptibility and the field direction H_0. The particle is subject to a torque τ of (31)

$$\tau = \frac{dE}{d\theta} = -E_{min}(2 \cos \theta \sin \theta) + E_{max}(2 \sin \theta \cos \theta) = (E_{max} - E_{min}) \sin 2\theta \tag{11}$$

which is sufficient to align both high and low spin microcrystals of ferric myoglobin along the field direction.

Unfortunately, it is not a simple matter to write a more exact expression for the torque in terms of the g tensor components, as suggested by our back-of-the-envelope calculations, since the high spin ferric iron is a ^{6}S Kramers ion, and the populations of the various energy levels, at room temperature, are not accurately known. Ferric iron microcrystals nevertheless order, as expected, with their low temperature maximum g value or maximum susceptibility along H_0, as will be shown below.

For cobalt systems, as discussed later in this publication, the situation is probably less complex and the torque can thus be written in terms of the susceptibilities

$$\tau = \tfrac{1}{2} H_0^2 \left(\frac{m}{M}\right) \left(\frac{\chi}{T}\right) (g_\parallel^2 - g_\perp^2) \sin 2\theta \tag{12}$$

where m is the particle mass, M the molecular weight, $g_\parallel$ and $g_\perp$ are the ESR g values parallel and perpendicular to H_0 and χ is the susceptibility.

We should add at this point that although magnetic ordering of a variety of both diamagnetic and paramagnetic systems has been known for many years (31-33), no NMR or ESR studies of ordered crystalline macromolecules have been reported to date.

We have not yet carried out successful electric ordering experiments; however, rough calculations indicate that the electric interactions may be comparable to typical magnetic interactions. The real situation is, however, quite complex since the field shapes and strengths in the microcrystals are quite difficult to calculate. Moreover, heating during ordering places severe restrictions upon sample conductivity. Although we have produced essentially insoluble protein crystals using glutaraldehyde cross-linking, the conductivity requirements for minimal heating but maximal electric field across the sample present severe experimental difficulties. We note later, however, that "mechanical" methods may also be used to produce microcrystal ordering.

Methods

Sperm whale (*P. catodon*) myoglobin was purified from Sigma Chemical Co. myoglobin (St. Louis, MO) (34) and freed of heme by extraction of a 2% protein solution at pH 3.5, 0.1 N in NaF, against 2-butanone (35). The apomyoglobin was extensively dialyzed, concentrated to 0.5 to 0.6 mM, and stored at 4°C. The CD_3I (Merck, Sharpe and Dohme, St. Louis, MO) had 0.95 mol fraction of ^{2}H. $^{13}CH_3I$ was from the Los Alamos Stable Isotope Research Resource and was kindly provided by Dr. B. Whaley and Professor N. Matwiyoff. All other chemicals were reagent grade. Distilled, deionized water was used throughout. Protein solutions were concentrated by ultrafiltration with a Diaflo apparatus (Amicon Corp., Lexington, MA) fitted with a UM-2 membrane.

Methylation of Apomyoglobin—The pH of the ~0.5 mM apomyoglobin was lowered to 4.0 with 0.1 N HCl. ^2H or ^{13}C-Labeled methyl iodide in a 100-fold M excess was added, and the two-phase solution was stirred at room temperature for 18 h in the dark. At the end of this period the clear, homogeneous solution was dialyzed against numerous changes of deionized water over a period of 24 h. The product obtained at this point contained *S*-methylmethionine residues almost completely replacing the methionine residues (36, 37). The solution of methylated protein was concentrated to 0.8 mM. The pH was adjusted with 5 N NaOH to 10.0 with rapid stirring at 0°C and then maintained between pH 9.5 and 11.5 by dropwise addition of 5 N NaOH during the addition of batches of mercaptoethanol (38) to a final concentration of 1.0 M (37). The final pH 10.0 solution was slightly turbid. After standing at 37°C for 18 h, it was dialyzed at room temperature against deionized water. The method used was thus as in Equation 13 and was similar to that used previously (36–38).

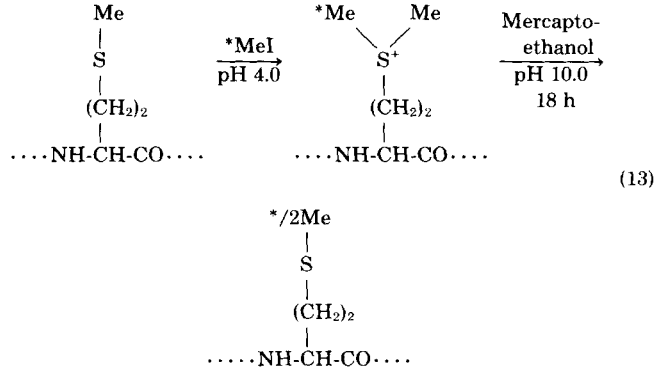

(13)

The apomyoglobins were rehemed by addition of a solution prepared by dissolving hemin chloride in 0.05 M NaOH, using a quantity that yielded the highest ratio of absorbance at 409 nm to that at 280 nm (measured at pH 6.5 in 0.1 M ionic strength phosphate buffer). The resulting red solution was dialyzed against water to approximately pH 8.0, and insoluble material was removed by centrifugation. The solution was concentrated by ultrafiltration and then brought to pH 6.35 with KH_2PO_4. The brown solution was chromatographed on a column of CM-50 Sephadex, equilibrated and eluted with pH 6.5 phosphate buffer at 0.1 ionic strength. The isotopically enriched myoglobin eluted at the same position as native myoglobin, leaving a second band at the origin. The eluted myoglobin was concentrated, deionized on freshly washed Rexyn I-300, and crystallized immediately.

Samples of labeled aquoferrimyoglobin (FeIII-H_2O), 2 to 4%, were crystallized from ~70% saturated ammonium sulfate that was weakly buffered to pH ~6.25 with 0.05 M disodium hydrogen orthophosphate (11). Crystals obtained were of the monoclinic form belonging to the space group $P2_1$ (type A) and in all cases were flattened on (001). Under the light microscope, the crystals appeared as prisms of widely varying dimensions, all less than ~0.3 mm. The crystals were filtered free of excess medium and spectra recorded as described below.

S-Me Methionine Synthesis—*S*-[*methyl*-$^2H_3$]methionine was prepared by refluxing 7 mmol of L-methionine (Sigma Chemical Company, St. Louis, MO) with 36 mmol of CD_3I in glacial acetic acid for 30 min. Solvent was removed *in vacuo* and the sulfonium salt recrystallized once from water-ethanol (1:10).

Nuclear Magnetic Resonance Spectroscopy—We used three "homebuilt" Fourier transform NMR spectrometers to record spectra. The first consists of an 8.5 Tesla 3.5-inch bore high resolution superconducting solenoid (Oxford Instruments, Osney Mead, Oxford, England) together with a variety of digital and radiofrequency electronics and a 400 kHz data acquisition system equipped with dual discs.[4] Spectra were recorded here using an 800-μl sample volume and a quadrature-echo (39) pulse sequence, using a 90° pulse width of between 3.5 and 9 μs. The spectrometer zero frequency was established using a 1% D_2O reference, the zero frequency for the protein samples investigated being set at about 2 ppm upfield from this position. The deuterium resonance frequency was 55.273 MHz. Additional ^2H spectra were recorded using the 5.2 Tesla widebore system described previously (40), using 7-μs pulse widths.

Carbon-13 NMR spectra were obtained at 33.7 MHz (corresponding to a magnetic field strength of 3.5 Tesla) under conditions of proton decoupling, using conventional Fourier transform methods. The multinuclear instrument described previously (24) was used. Spectra were recorded using a quadrature detection scheme (Nicolet software package FT-74Q) with 20 kHz spectral widths. The 90° pulse width was generally ~12 μs for a 1-ml sample. Carbon-13 chemical shifts were measured with respect to an internal reference sample of 1,4-dioxane.

Due to the extreme heating of samples containing ~90% saturated aqueous ammonium sulfate during acquisition of ^1H-decoupled carbon-13 Bloch decays, we used ~150 watts of proton radiofrequency decoupling power (at 150.00 MHz) gated "on" for only 50 ms (the acquisition time) every 4 s (the recycle time or period of the experiment). This corresponds to only about a 2-watt average power dissipation. Nevertheless, it was found to be desirable to cool the sample with a very rapid stream of cool air in order to prevent protein denaturation. The probe used was a double-tuned single-turn solenoid design using 1/4 wave elements (41). We used in addition a high power tubular lowpass filter, having ~100 db attenuation at 150 MHz, on the input to the preamp to prevent leakage of 150 MHz radiation into the receiver system.

Electron Spin Resonance Spectroscopy—ESR spectra were recorded using a Varian Instruments (Palo Alto, CA) 9.3 GHz E-4 spectrometer at a variety of modulation amplitudes and power levels. The sample temperature could be varied down to ~4.2°K using an Oxford Instruments (Osney Mead, Oxford, U.K.) Heli-Trans System.

Spectral Simulations—Spectral simulations were carried out on the University of Illinois Digital Computer Laboratory's Control Data Corporation Cyber-175 system, which is interfaced to a Tektronix 4006 graphics terminal and interactive digital plotter (Tektronix, Beaverton, OR) in our laboratory.

Efficient quadrupole relaxation is expected to give a Lorentzian contribution to the ^2H-NMR linewidth, leading to the powder pattern lineshape shown in Equation 14 and Fig. 1*A*, where δ is the half-width at half-height of the Lorentzian broadening function,

$$g(\omega, \Delta\nu_Q) = \int_0^{\pi/2} (d\theta \sin\theta)(\delta/\pi)/(\delta^2 + (\omega \pm (\Delta\nu_Q/2) \times (3\cos^2\theta - 1))^2) \quad (14)$$

and $\Delta\nu_Q$ is the quadrupole splitting. Axially symmetric carbon-13 lineshapes correspond to just one-half of the ^2H-powder pattern (Fig. 1*D*). For ordered systems there is simply a Lorentzian line at a frequency ω corresponding to the appropriate θ. An asymmetry parameter η ($(V_{xx} - V_{yy})/V_{zz}$) may be introduced into Equation 14 to calculate $\eta \neq 0$ ^2H lineshapes, axially asymmetric ^{13}C-powder patterns and, in general, ESR lineshapes; however, the resulting lineshape equations are even more complex, and the interested reader is referred to References 42 and 43.

RESULTS AND DISCUSSION

We show in Fig. 2 deuterium NMR spectra, obtained by the Fourier transform method at 55.3 MHz (corresponding to a magnetic field strength of about 8.5 Tesla or 85,000 G), of *S*-[*methyl*-$^2H_3$]methionine iodide (Fig. 2*A*) and [C^ϵ-$^2H_3$]-labeled methionine (Fig. 2*C*), together with the theoretical ^2H-NMR lineshapes expected for spin $I = 1$ nuclei having asymmetry parameters $\eta = 0$ and corresponding to the observed quadrupole splittings for *S*-Me-Met (42 kHz, Fig. 2*B*) and ^2H-Me-Met (40.5 kHz, Fig. 2*D*). These results show the type of spectra expected for labeled methyl groups undergoing fast rotation about the C_3 axis (44, 45), where "fast" is $\gtrsim 10^6$ s^{-1}. In the absence of fast motion a powder pattern having a breadth of ~125 kHz would be observed (44, 45). Fast rotation reduces this breadth by a factor of $1/2(3\cos^2\theta - 1)$, where θ is the angle between the axis of internal rotation and the principal axis of the electric field gradient tensor (the C—D bond vector). For a tetrahedral CD_3 group this factor is −0.33, which would result in an observed $\Delta\nu_Q$ of ~42 kHz, essentially that observed in Fig. 2, *A* and *B*, assuming a value for the electric quadrupole coupling constant of ~170 kHz (44) and $\eta = 0$. Although there are likely to be small deviations in e^2qQ/h and θ from the values assumed above, due to bonding to sulfur, the spectra of Fig. 2 give a yardstick with which to compare results obtained on protein systems. Please note,

[4] R. Jacobs, C. Reiner, and E. Oldfield, unpublished results.

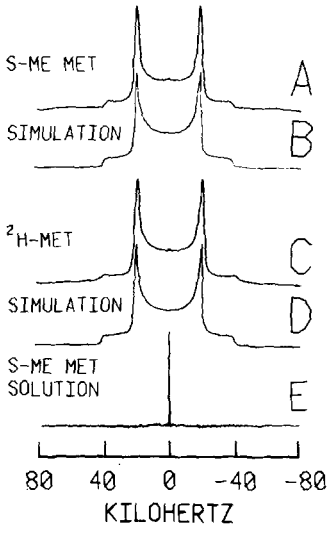

FIG. 2. **Deuterium quadrupole echo Fourier transform NMR spectra at 55.3 MHz and 24 ± 1°C of S-methylmethionine and methionine labeled as C^2H_3 in the methyl group.** *A*, S-[*methyl*-$^2H_3$]methionine, 512 scans, 300 ms recycle time, $\tau_1 = \tau_2 = 80$ μs, 9 μs 90° pulse widths, 167 kHz spectral width, 4096 real data points, 200 Hz line broadening. *B*, spectral simulation of *A* using $\Delta\nu_Q = 42$ kHz, $2\delta = 1.2$ kHz. *C*, C^ϵ-$^2H_3$-labeled methionine, 86 scans, 990 s recycle time, $\tau_1 = \tau_2 = 80$ μs, 9 μs 90° pulse widths, 167 kHz spectral width, 4096 real data points, line broadening = 200 Hz. *D*, spectral simulation of *C* using $\Delta\nu_Q = 40.5$ kHz, $2\delta = 1.2$ kHz. *E*, solution spectrum of sample of figure of part *A*, ~50 mg in 1 ml of deuterium-depleted H_2O, 20 scans, 1 s recycle time, 9-μs 90° pulse width, other conditions as in *C*.

however, that we do not need to know the exact value of the electric quadrupole coupling constant (e^2qQ/h) in order to obtain structural information in oriented proteins since the powder and oriented spectra are all that are required to determine θ information, as discussed below. Determination of (e^2qQ/h) in the absence of methyl group rotation would, however, permit determination of the C^2H bond angle, Φ (45).

For comparison with the solid state spectra of Fig. 2 we present in Fig. 2*E* a spectrum of *S*-[*methyl*-$^2H_3$]methionine in aqueous solution. In the presence of fast isotropic motion the time average value of $3\cos^2\theta - 1$ in Equation 5 is zero, hence a narrow Lorentzian absorption at $\omega = 0$ is observed, Fig. 2*E*. Depending on the precise details of the rates and types of motions undergone by a methionine methyl group in a protein crystal, we could expect any spectrum intermediate between those shown in Fig. 2. Such intermediate lineshapes may be calculated using for example the methods of Freed (46). It is worth noting at this point that the spin lattice relaxation time of methionine is quite long, ~45 s, while that of *S*-Me methionine is relatively short. Attempts to acquire methionine data with much shorter recycle times resulted in highly distorted spectra. T_1 contributions to δ are, however, insignificant in both instances.

^{2}H-NMR of Proteins—A spectrum of lyophilized [C^ϵ-$^2H_3$]methionine myoglobin, labeled at positions Met-55 and Met-131, is shown in Fig. 3*A*. This spectrum is somewhat similar to that seen with the free amino acid (Fig. 2*C*) except for a reduction in quadrupole splitting ($\Delta\nu_Q$) to 35 kHz and a large increase in linewidth (W, 2δ), from 1.0 to 6.6 kHz (Table I). The spectrum of hydrated protein crystals, Fig. 3*B*, shows an additional decrease in $\Delta\nu_Q$ and W (Table I). Natural abundance ^{2}H background signals contribute little to the observed ^{2}H-NMR spectra, as expected, and a reference "blank" for the hydrated protein sample is shown in Fig. 3*C*.

The above results strongly suggest that there are medium amplitude fluctuations of the S^δ—C^ϵ bond vector in the lyophilized protein crystal at 21°C which are absent in the free amino acid, as evidenced by the decrease in $\Delta\nu_Q$ from 40.5 to 35 kHz, and that hydration with 3.2 M ammonium sulfate increases the amplitude of these fluctuations, as evidenced by the additional decrease in $\Delta\nu_Q$ to 31 kHz.

The spectrum of the hydrated protein crystals of Fig. 3*B* may be quite well simulated by using a $\Delta\nu_Q$ of 31.0 kHz, but improved agreement is obtained by using in addition an asymmetry parameter $\eta \sim 0.15$. Alternative simulations using $\eta = 0$ and two different $\Delta\nu_Q$ values (corresponding to inequivalent motions for Met-55 and Met-131) give poorer agreement. It is, therefore, possible that the S^δ—C^ϵ vector undergoes some type of specialized restricted or jump motions causing a nonzero asymmetry parameter, but we cannot detail

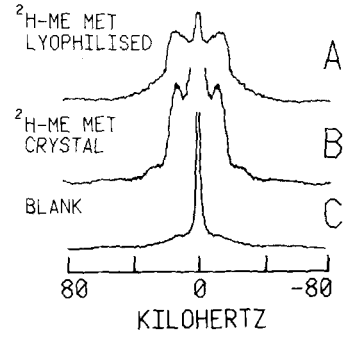

FIG. 3. **Deuterium quadrupole echo Fourier transform NMR spectra at 55.3 MHz of ^{2}H-methyl labeled and nonlabeled myoglobin.** *A*, ^{2}H-methyl labeled metaquomyoglobin, lyophilized sample, 18 ± 1°C, 697,473 scans, 65 ms recycle time, $\tau_1 = \tau_2 = 61$ μs, 8 μs 90° pulse widths, 167 kHz spectral width, 4096 real data points, 400 Hz line broadening. *B*, ^{2}H-methyl-labeled metaquomyoglobin microcrystals hydrated with ~90% saturated $(NH_4)_2SO_4$, pH = 6.25, 19 ± 1°C. 176,685 scans, 65 ms recycle time, $\tau_1 = \tau_2 = 65$ μs, 7 μs 90° pulse widths, 4096 real data points, 400 Hz line broadening. *C*, nonlabeled metaquomyoglobin microcrystals hydrated with 90% saturated $(NH_4)_2SO_4$, 20 ± 1°C. 581,994 scans, 65 ms recycle time, $\tau_1 = \tau_2 = 63$ μs, 7 μs 90° pulse widths, 167 kHz spectral width, 4096 real data points, line broadening = 400 Hz. The natural abundance protein ^{2}H contribution to the spectra of *A* and *B* is insignificant.

TABLE I

Deuterium NMR quadrupole splitting and linewidth parameters for labeled amino acid and Physeter catodon myoglobin powders at several temperatures

Data were obtained at a magnetic field strength of 8.5 Tesla (corresponding to a ^{2}H resonance frequency of 55.3 MHz). Typical spectra are shown in Figs. 2, 3, 6, 8, and 11. Simulations were carried out using Equation 14.

System	Quadrupole splitting	Linewidth
	$\Delta\nu_Q$, kHz[a]	W, 2δ, kHz[b]
S-[*methyl*-$^2H_3$]methionine[c]	42.0	1.0
[C^ϵ-$^2H_3$]methionine[c]	40.5	1.0
Lyophilized [^{2}H]Mb[c, d, e]	35.0	6.6
Lyophilized [^{2}H]Mb (−30°C)[d, e]	40.5	5.6
Hydrated [^{2}H]Mb[c, d, e, f]	31.0	2.4
Hydrated [^{2}H]Mb (−30°C)[d, e, f]	38.0	2.4

[a] Obtained from a spectral simulation. Error is ±500 Hz.

[b] Obtained from a spectral simulation and corrected for instrumental broadening due to exponential multiplication. Error is ±15%.

[c] Obtained at ambient temperature of 22 ± 3°C.

[d] Labeled as C^ϵ-$^2H_3$ at the methyl groups of methionine-55 and methionine-131. See under "Experimental Procedures" for details.

[e] Metmyoglobin, containing a high or mixed spin ferric iron atom, water ligand.

[f] Hydrated sample prepared by crystallizing metaquomyoglobin from 3.2 M ammonium sulfate, then removing excess mother liquor by filtration.

them as yet. On cooling the sample of Fig. 3*B* to −38°C, zero asymmetry parameter spectra are regained. These results indicate that both relatively high temperatures (24°C) and hydration are required for these motions, but further work is clearly required in order to gain a full understanding of the details of the ^{2}H-NMR lineshapes of systems undergoing restricted motion (46).

We feel that it is nevertheless instructive to try to detail the off axis methyl group motions in terms of a Gaussian distribution and an order parameter model. We will thus use the following expression to deduce an order parameter, S_α, for the methyl group motion, by analogy with Equation 23 of Reference 40

$$\Delta\nu_Q = \frac{3}{16}\left(\frac{e^2qQ}{h}\right)\overline{(3\cos^2\alpha - 1)}\,\overline{(3\cos^2\gamma - 1)}(3\cos^2\theta' - 1) \qquad (15)$$

where α, γ, and θ' are shown in Fig. 4. We define a new symmetry axis as d, the director axis (Fig. 4), θ' is the angle between the director d and the magnetic field H_0, α is the instantaneous angle between the S^δ—C^ϵ bond vector and the director and γ is the S^δ—C^ϵ—^{2}H bond angle. If this approach is used, it is a simple matter to deduce an order parameter $S_\alpha = \frac{1}{2}(3\cos^2\alpha - 1) = 0.76$ for the order parameter of the S^δ—C^ϵ bond vector in the hydrated protein crystal, Fig. 3*B*. Using the models outlined previously (40, 47) this can be shown to correspond to a most probable angle of tilt α_0 (assuming an axially symmetric Gaussian distribution function) of ~17°. This reduces to about 8° for the low temperature hydrated sample. Although these values should be regarded as very approximate, they do clearly show large motional changes in the protein crystal due to hydration and to relatively small changes in temperature on the timescale of $\sim 10^{-5}$ s. However, we have obtained no information on the orientation of the methionine methyl groups in the protein crystal and have not yet resolved the two nonequivalent labeled sites, Met-55 and Met-131.

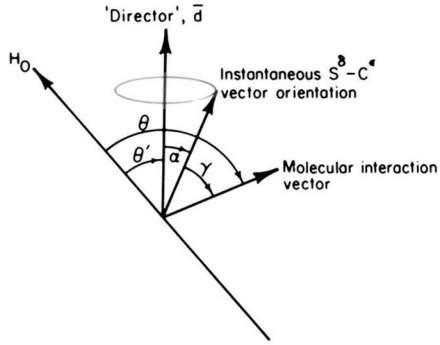

FIG. 4. **Angle and vector designations used in the text to describe the off axis motion of the *S*-methyl group in labeled myoglobin.**

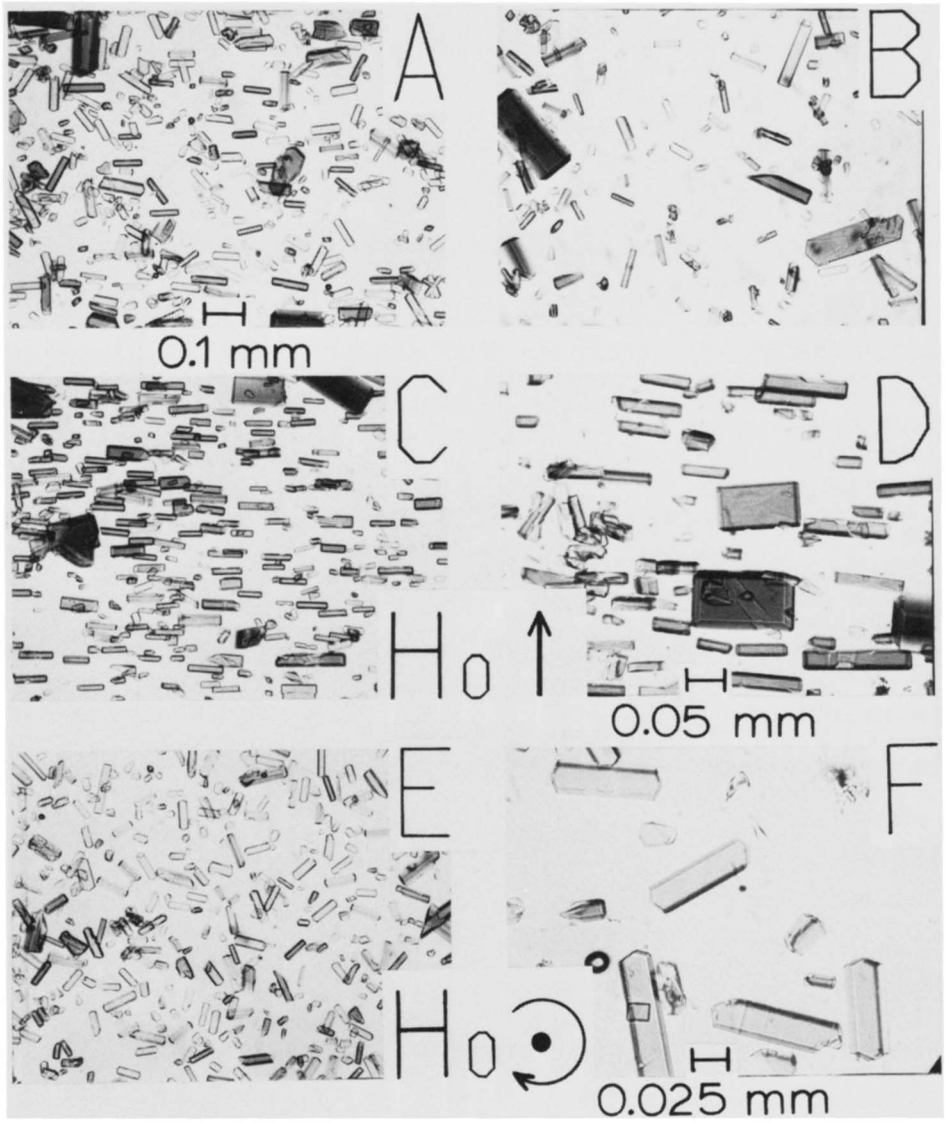

FIG. 5. **Photomicrographs of sperm whale (*Physeter catodon*) metaquomyoglobin microcrystals suspended in ~90% saturated $(NH_4)_2SO_4$.** *A*, random microcrystals in the absence of a magnetic field, ×100 on a 5 × 4 inch Polaroid negative. *B*, random microcrystals, ×200. *C*, ordered microcrystals, ×100. The sample was magnetically ordered in a field of 0.3 Tesla for approximately 20 min. The field direction is indicated in the figure. *D*, as *C* but ×200. *E*, magnetically ordered protein microcrystals, ×100. The axis of ordering is perpendicular to the plane of the page and is approximately along the crystallographic c^* axis. *F*, high power (×400) view of *E*. The pointed ends of the crystals can clearly be seen in *F*, and the square ends may be seen in *D*. In both instances the crystals are ordered along the crystallographic c^* axis.

Magnetic Ordering—As discussed above, we have obtained highly ordered arrays of paramagnetic protein microcrystals by means of a magnetic ordering method which permits us to obtain single crystal orientation NMR spectra of protein microcrystals.

We show in Fig. 5, *A* and *B*, photomicrographs of a randomly oriented array of microcrystals of metaquomyoglobin (from sperm whale) crystallized from 3.2 M $(NH_4)_2SO_4$ as discussed under "Experimental Procedures," which has been suspended in a dense (~90% saturated) ammonium sulfate solution. Fig. 5*A* shows a wide field view (×100 on a 5 × 4 inch Polaroid negative), and Fig. 5*B* is from the same sample but at higher magnification (×200) and includes several larger crystals (~0.2 mm length). Careful inspection of Fig. 5, *A* and *B*, reveals two apparent crystal types, those with square and those with pointed ends.

When the sample of Fig. 5, *A* and *B*, is placed in a direct current magnetic field (H_0) of about 0.3 Tesla strength the protein microcrystals become highly ordered, aligning with their long axis perpendicular to the field direction (Fig. 5, *C* and *D*). Note that now all crystals appear to have square ends.

Clearly then, the paramagnetic protein microcrystals are being aligned by the field and must thus have their maximum (crystal) susceptibility along H_0, which as shown by Fig. 5, *C* and *D*, corresponds to the crystallographic c^* axis along H_0. This is the result that might be predicted on the basis of the ESR (14) and crystal structures (11, 48) if only the lowest Kramers levels were populated. We discuss this latter point in more detail later in this publication. In any case, it appears from Fig. 5, *A* to *D*, that there is only one crystal habit in our sample; when viewed along the *a* axis the crystal appears rectangular (Fig. 5, *C* and *D*), but in a random powder distribution views both along c^* (Fig. 5, *A* and *B*, pointed ends), *a* and *b* (Fig. 5, *A* and *B*, square or rectangular) will be seen. Our sample holder geometry for photomicrography consists of a thick microscope slide assembly and thus tends to flatten crystals so end-on views are seen only for smaller crystallites.

A prediction of the above is that if crystals are aligned and viewed along the field direction (approximately along c^*) then they will all appear with pointed ends. This indeed occurs, and results are shown in Fig. 5, *E* and *F*. Here, we simply oriented a sample suspended in a vertical microscope cavity slide in a horizontal direct current magnetic field of ~3kG, then removed it and viewed it in the normal horizontal fashion. The result is a view along the field direction, Fig. 5, *E* and *F*. Note all crystals are capped in Fig. 5*F* while all ends appear square in Fig. 5*D*, and the sample is disordered along c^*.

In Fig. 6 we show the effects on the ^{2}H-NMR spectra of suspending microcrystals of aquoferrimyoglobin and allowing them to be ordered under the influence of the external magnetic field. We show first for comparative purposes in Fig. 6*A* a "powder" spectrum of aquoferrimyoglobin microcrystals. The microcrystals form a solid disordered mass after removal of saturated ammonium sulfate solution by filtration. The spectrum of Fig. 6*A*, as discussed above, may be attributed to two overlapping powder patterns having a quadrupole splitting ($\Delta\nu_Q$) of 31 kHz, as shown in Fig. 6*B*. At low temperatures ($\lesssim$−30°C) $\eta = 0.08$ spectra having $\Delta\nu_Q$ ~38 kHz are obtained (see Table I).[5] By contrast to the powder spectrum of Fig. 6*A*, a very narrow-line spectrum having $\Delta\nu_Q = 53.6$ kHz is obtained when the microcrystals of Fig. 6*A* are resuspended in ^{2}H-depleted 90% saturated ammonium sulfate (pH 6.3), which has the same density as the crystals, Fig. 6*C*. This spectrum has a $\Delta\nu_Q$ much greater than the ≈40 kHz expected for only methyl group rotation (Fig. 2, *A* and *C*) and does not have the appearance of a normal powder pattern, Fig. 1*A*. Rather, it closely resembles the theoretical single crystal orientation spectrum of Fig. 1*B*. The spectrum of Fig. 6*C*, therefore, indicates that "pseudo-single crystal" NMR spectra of paramagnetic proteins may be readily obtained by means of the magnetic ordering effect. From the result of Fig. 6*C* it follows that θ' for at least one methionine S^δ—C^ϵ vector is 17.5 ± 2°, as shown in Fig. 6*D*. The results of sample freezing and additional pH dependence experiments, in which crystal orientation is changed by means of a spin-state transition[5] indicates that a second methionine resonance lies under the HO^2H resonance. Thus θ' for this group is 54.7 ± 2°. These results represent the first direct determination by NMR spectroscopy of a structural parameter in a protein crystal. Freezing experiments (see below) also rule out motional narrowing of the quadrupole interaction by particle oscillation, since sharp spectra of the same $\Delta\nu_Q$ are obtained even on frozen samples.

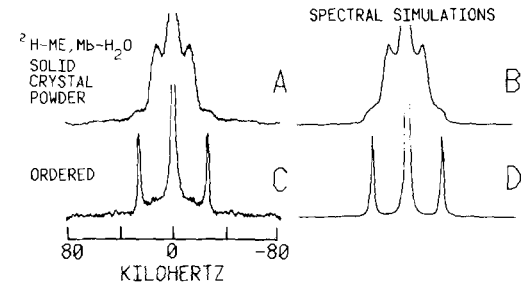

FIG. 6. **Deuterium quadrupole echo Fourier transform NMR spectra at 55.3 MHz and 20 ± 2°C of ^{2}H-methylmethionine labeled sperm whale myoglobin as a solid hydrated crystal powder, and a magnetically ordered sample, together with their spectral simulations.** *A*, solid crystal powder hydrated with ~90% saturated $(NH_4)_2SO_4$. 176,685 scans, 65 ms recycle time, $\tau_1 = \tau_2 = 65$ μs, 7 μs 90° pulse widths, 167 kHz spectral width, 4096 real data points, line broadening = 400 Hz. *B*, spectral simulation of *A* using $\Delta\nu_Q = 31.0$ kHz, $\eta = 0.15$, $2\delta = 2.8$ kHz. *C*, magnetically ordered spectrum of the sample of *A* after suspension in ~90% saturated $(NH_4)_2SO_4$. 245,839 scans, 65 ms recycle time, $\tau_1 = \tau_2 = 61$ μs, 7 μs 90° pulse widths, 167 kHz spectral width, 4096 real data points, line broadening = 400 Hz. *D*, spectral simulation of *C* using $\Delta\nu_Q = 53.6$ kHz, 2δ (outer component) = 2.4 kHz. The inner methionine resonance cannot be accurately simulated due to the overlapping resonance from natural abundance HO^2H.

Further evidence for the macroscopic magnetic ordering origins of the sharp line spectrum shown in Fig. 6*C* is given in Figs. 7 and 8. In Fig. 7 we show, schematically, the effects on the ^{2}H-NMR lineshape expected for three cases of rotation of a frozen, magnetically oriented sample. In Fig. 7*A* we show a static C^2H vector orientation (equivalent to the S^δ—C^ϵ vector orientation in the case of fast methionine methyl group rotation where a new effective field gradient tensor is produced) oriented along the magnetic field direction, H_0. In this case $\theta' = 0°$ and a quadrupole splitting of $\Delta\nu_Q$ ~276 kHz would be expected in the case of an aromatic system undergoing no motion (26), for example a heme meso ^{2}H-atom, or ≈64 kHz for the case of the rotating S—C^2H_3 group in a protein crystal. Such broad splittings are indeed obtained for ^{2}H-labeled hemes.[6] Rotation of the sample through 90° about any axis in the *x*-*y* plane results in all electric field gradient tensor principal axes lying in the *x*-*y* plane, at 90° to H_0, Fig. 7B. A sharp line spectrum having $\Delta\nu_Q$ ~138 kHz (aromatic ring, no motion) or ≈32 kHz (fast methyl rotation) is thus produced, as shown in Fig. 7*B*. Note, of course, that a sample magnetically ordered along *z* will be rotationally disordered about *z*, since in the absence of any other interactions all such orientations are degenerate.

[5] T. M. Rothgeb and E. Oldfield, unpublished results.

[6] R. Lee and E. Oldfield, unpublished data.

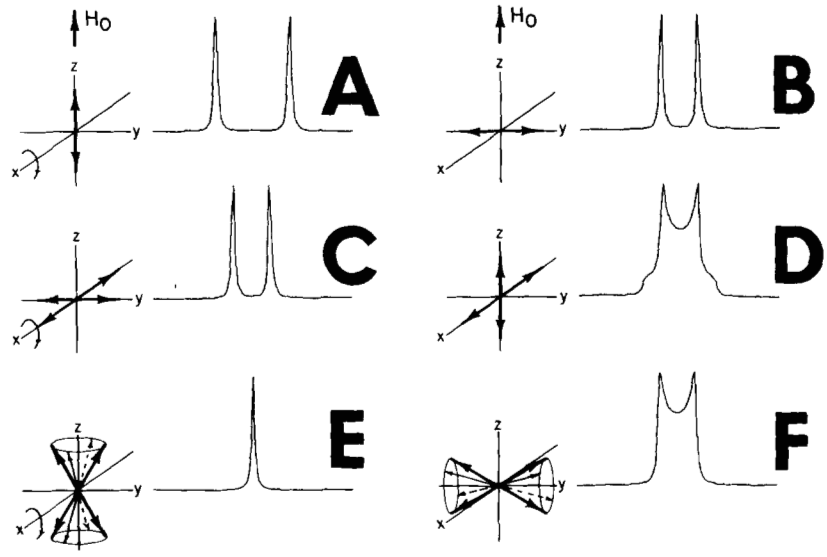

FIG. 7. **Vector diagram and computer-simulated results showing the effects of sample rotation on ^{2}H-NMR spectral appearance for various initial conditions.** *A*, principal electric field gradient tensor components aligned along the field direction H_0. *B*, vector orientation and spectral appearance after a 90° rotation about the *x* axis. *C*, principal electric field gradient tensor components oriented at 90° to the field direction H_0, *i.e.* electric field gradient principal components oriented or lying in the *xy* plane. *D*, vector orientation and spectral appearance after a 90° rotation around *x*. Note that a powder pattern having the full spectral breadth is obtained although the perpendicular edges are somewhat attenuated. *E*, electric field gradient tensor principal components oriented at the magic angle (54.7°) to the field direction H_0. An isotropic narrow Lorentzian absorption is obtained. Note that the vectors are oriented on the surface of a cone. *F*, vector orientation and spectral appearance after 90° rotation of the array shown in *E*, about the *x* axis. A complex tilted conical distribution function lineshape is generated.

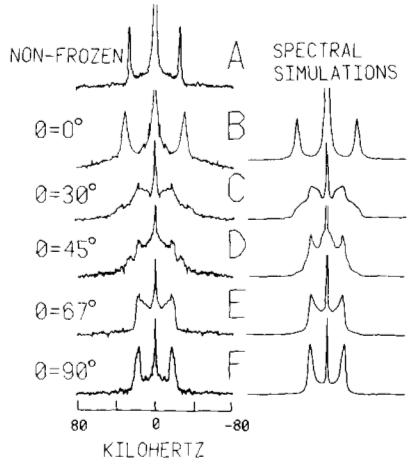

FIG. 8. **Solution and frozen sample ^{2}H-NMR rotation patterns of ^{2}H-methylmethionine labeled ferrimyoglobin from sperm whale.** *A*, nonfrozen sample, spectral conditions as in Fig. 6*C*. *B* to *F*, frozen samples rotated about an axis perpendicular to the field direction by the amount indicated. Data acquisition conditions were typically recycle time = 65 ms, $\tau_1 = \tau_2 = 65$ μs, 7 μs 90° pulse widths, 167 kHz spectral width, 4096 real data points, 400 Hz line broadening due to exponential multiplication. The number of scans varied between 82,615 and 262,000. The spectral simulations assumed $\theta_1 = 17.5°$, $\theta_2 = 54.6°$, $2\delta = 4.4$ kHz, and $\Delta\nu_Q = 38$ kHz. The rotation angles are accurate to ±3°. A small isotropic component was also included in the simulation.

A sample giving rise to a $\theta' = 90°$ magnetically ordered spectrum (Fig. 7*C*) having $\Delta\nu_Q \sim 138$ kHz for the case of for example a rigid heme group or ≈32 kHz in the case of fast methyl group motion in the protein, will, however, have a complete *x*-*y* distribution of orientations (Fig. 7*C*), although the observed spectrum will be identical with that observed in Fig. 7*B* which originates from the unique distribution shown. Rotation of the *x*-*y* powder distribution shown in Fig. 7*C* through 90° about any axis orthogonal to *z* generates the same distribution, now in the appropriate *z*-*x*, *z*-*y*, or other plane. The result is that a new powder spectrum is generated having all frequency components, from $+\omega_\parallel$ to $-\omega_\parallel$, as shown in Fig. 7*D*.

Any group not undergoing fast isotropic motion but still showing a zero quadrupole splitting, Fig. 7*E*, must be oriented at the magic angle (54.7°) to the field, such that $(3\cos^2\theta' - 1) = 0$. Such groups must be oriented through the sample on the surface of a cone, so upon rotation a complex tilted conical distribution (Fig. 7*F*) powder pattern lineshape must be calculated. The result is shown. It is clear from the results of Fig. 7 that computer simulations are necessary for all but the simplest sample rotation experiment.

A microcrystalline sample of aquoferrimyoglobin, labeled as C^2H_3 at C^ϵ of Met-55 and Met-131, was magnetically ordered at 8.5 Tesla for 30 min at 18°C, to produce a highly oriented specimen. The sample was then frozen by passing a stream of cold nitrogen through the NMR probe. The sample was completely solid at −30°C, the temperature of the ^{2}H-NMR experiment.

As may be seen from the results of Fig. 8, A and *B*, the transition from a state in which the protein microcrystals are suspended in 90% saturated ammonium sulfate (Fig. 8*A*) to the frozen state (Fig. 8*B*) results in only a minor change in $\Delta\nu_Q$ (31 to 38 kHz), and this change does in fact occur gradually and does not appear to correlate with bulk-phase-water freezing. It thus seems safe to assume that any changes in crystal structure are very minor on freezing.

On rotating the frozen sample of Fig. 8*B* about an axis orthogonal to H_0, very dramatic changes in the ^{2}H-NMR spectrum are seen (Fig. 8, *C* to *F*). We show in Fig. 8, in addition to the experimental results, computer simulations of the experimental data made assuming methionine methyl groups having $\theta = 54.7°$ and 17°, and the tilt angles $\zeta = 0°$, 30.0°, 45°, 67.5°, and 90°, as shown in the figure. A linewidth (2δ) of 4.4 kHz and a $\Delta\nu_Q$ of 38 kHz were used in the spectral simulations (Table II). The theoretical results are in general in excellent agreement with the experiment findings and confirm the idea that the samples were ordered by the intense

TABLE II

Deuterium NMR quadrupole splitting and linewidth parameters for magnetically ordered ^2H-labeled Physeter catodon ferrimyoglobins

Samples were ordered and data obtained at a magnetic field strength of 8.5 Tesla. Typical spectra are shown in Figs. 6, 8, and 11.

System	Quadrupole splitting	Linewidth
	$\Delta\nu_Q$, kHz[a]	W, 2δ, kHz[b]
Random metaquo[^{2}H]Mb[c, d, e]	31.0	2.4
Ordered metaquo[^{2}H]Mb[c, d, f]	0, 53.6	2.0[g]
Random cyanomet[^{2}H]Mb[c, e, h]	33.0	2.4
Ordered cyanomet[^{2}H]Mb[c, f, h]	13.6, 38.1	2.0
Metaquo[^{2}H]Mb, rotation pattern[d, i]		4.0

[a] Obtained from a spectral simulation. Error is ±500 Hz.

[b] Obtained from a spectral simulation and corrected for instrumental broadening due to exponential multiplication. Error is ±15%.

[c] Data were recorded at ambient probe temperature of 22 ± 3°C.

[d] [^{2}H]Me-labeled aquoferrimyoglobin, pH ~6.3. Protein is labeled solely at Met-55 and Met-131 C^ϵ.

[e] Sample has been filtered free of 3.2 M $(NH_4)_2SO_4$ mother liquor and packed into an NMR tube. Sample did not lose water during data acquisition.

[f] Sample is suspended in ~90% saturated $(NH_4)_2SO_4$.

[g] Only the outer line was simulated. The inner ($\Delta\nu_Q$ ~0) line may have a different width.

[h] ^{2}H-Me-labeled cyanometmyoglobin, pH ~6.4. Labeled at Met-55 and Met-131 only.

[i] Sample was ordered at 8.5 Tesla at ~24°C, then rapidly cooled to −30°C with a cold N_2 gas stream. The sample appeared to freeze at ~−25°C. Slow sample cooling caused formation of a powder spectrum (without sample rotation) due to $(NH_4)_2SO_4$ crystallization resulting in a solvent density decrease and protein sedimentation.

magnetic field. Simulations using only orientations of 54.7 or 17° did not give good agreement with experiment.[5]

Carbon-13 NMR—The production of high sensitivity high resolution magnetic resonance spectra and the derivation of both static and dynamic information about protein structure should not be confined to deuterium NMR. We have, therefore, synthesized [C^ϵ-$^{13}CH_3$]methionine-labeled myoglobin, labeled at both positions Met-55 and Met-131 with ^{13}C, and have obtained high resolution spectra of magnetically ordered samples, as shown in Fig. 9. In the absence of an intense proton-decoupling field both $\mathcal{H}_{DD}$ and $\mathcal{H}_{CSA}$ (Equation 1) lead to severe line broadening, and it is not possible to resolve the two individual methionine resonances, even in a magnetically ordered sample (Fig. 9*A*). In the presence of intense decoupling, but in the absence of magnetic ordering, it is again not possible to obtain resolved resonances, since $\mathcal{H}_{CSA}$ now dominates, and the methionine methyl group resonances are spread over some 40 ppm or ~1500 Hz. Upon magnetic ordering, however, the two resonances are resolved in a ^{1}H-decoupled spectrum as shown in Fig. 9*B*, and this resolution can be improved considerably by convolution difference spectroscopy (21, 22) as shown in Fig. 9*C*. The two resonances are separated by 9.3 ppm in the microcrystalline protein sample, occupying different parts of a chemical shift anisotropy powder pattern due to their different orientations in the protein crystal. In addition there may be hyperfine contributions to these shifts in the crystalline solid state.[6] In solution these two resonances are separated by about 1 ppm (36, 37).

These results indicate that high resolution carbon-13 NMR spectra of protein crystals may be obtained and suggest that in addition the orientations of carbon-13-containing residues may be deduced. In a later paper we will show how these resolved resonances may be specifically assigned to Met-55 and Met-131.

Electron Spin Resonance Spectra—We have shown in Figs. 6, 8, and 9 that it is possible to obtain high resolution solid state ^{2}H- and ^{13}C-NMR spectra of labeled protein crystals containing a high spin ferric iron ($S = 5/2$) by means of the magnetic ordering effect. We would, therefore, predict that it should be possible to obtain similar high resolution electron spin resonance spectra of these same crystals. This prediction is borne our experimentally, as shown in Fig. 10.

In Fig. 10*A* we present the 9.3 GHz continuous wave electron spin resonance spectrum (at 12°K) of a powder sample of specifically deuterated metmyoglobin, and in Fig. 10*B* we show an ESR spectrum of the same sample after being magnetically ordered at 0.9 Tesla for 15 min at 20°C, then cooled to 6°K. The spectrum of Fig. 10*A* obviously corresponds to a normal high spin ferric iron powder pattern signal having $g_\perp = 6.0$ and $g_\parallel = 2.0$. It is assumed that the lowest doublet is $S_z = \pm 1/2$ with a zero field splitting to the other spin doublets much greater than that of the microwave quanta (14). The

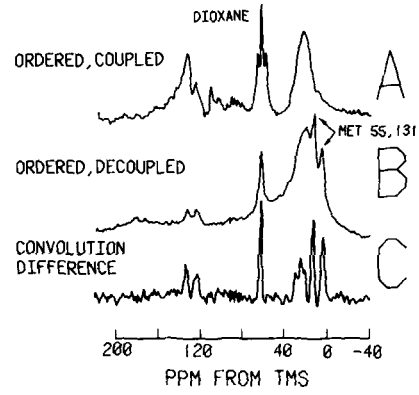

FIG. 9. **Carbon-13 Fourier transform NMR spectra at 37.7 MHz of ^{13}C-methylmethionine labeled sperm whale aquoferrimyoglobin microcrystals in a magnetically ordered sample.** *A*, coupled spectrum, crystals ordered at 3.5 Tesla, pH = 6.25, 4.1 s recycle time, 110 μs data acquisition delay, 12 μs 90° pulse width, 20 kHz spectral width, 4096 complex data points, 30 Hz line broadening. *B*, fully proton-decoupled spectrum. Other conditions as in *A*, except for a 30-μs data acquisition delay time and 10-μs 90° pulse width. *C*, convolution difference spectrum of B using $w_1 = 30$ Hz, $w_2 = 300$ Hz. Chemical shifts are in ppm from internal 1,4-dioxane.

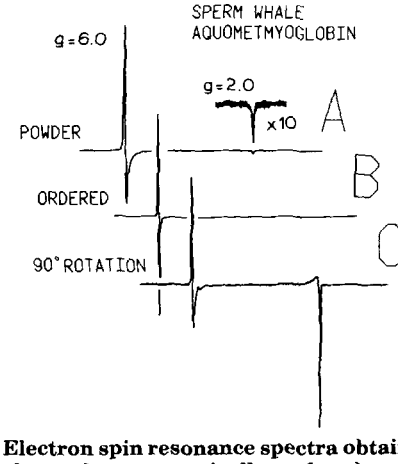

FIG. 10. **Electron spin resonance spectra obtained at 9.3 GHz of hydrated powder, magnetically ordered, and rotated-ordered sperm whale aquoferrimyoglobin microcrystals.** *A*, random powder sample hydrated with 90% saturated $(NH_4)_2SO_4$, pH (at 24°C) = 6.25, 1.25 G modulation amplitude, 100 kHz modulation frequency, 12°K, 1.0 milliwatt microwave power. *B*, sample magnetically ordered at 9 kG then rapidly frozen, 0.32 G modulation amplitude, 100 kHz modulation frequency, 5.5°K, 0.2 milliwatt microwave power. *C*, spectrum of sample of *B* after a 90° rotation about an axis orthogonal to that of ordering. Same spectrometer conditions as in *B*. Note the large $g = 2$ component in the rotated sample, *C*. The sample of *B* orders along a low temperature $g = 6$ axis.

spectrum of Fig. 10*A* is essentially identical with that of Hori (49). In contrast, the spectrum of Fig. 10*B* shows a very symmetric derivative absorption centered at a g value of 6.0, with only a very small component at a g value of 2.0. The spectrum of Fig. 10*B* corresponds, therefore, to ferrimyoglobin molecules oriented with their maximum g value (~6) along the field direction, together with a very small contribution from less well ordered material (at a g of 2). This $g = 2.0$ component is even smaller in a sample which has been oriented at 8.5 Tesla, then frozen for ESR.[5] This result is that expected from Equation 12 where we show that the torque on a particle depends on the square of the magnetic field strength. At 8.5 Tesla it is likely that even the smallest particles in our sample are well ordered by the field. Similar magnetic orientation of highly paramagnetic low molecular weight species has been observed previously in ESR spectroscopy (31) and in the analogous technique of far-infrared magnetic resonance (33), although in both instances only small inorganic model complexes were investigated.

These results together with those of Fig. 5 indicate that the metaquomyoglobin crystals are magnetically ordered along the crystallographic c^* axis, and from Fig. 10 we see, at least at liquid helium temperatures, that this axis corresponds to one of the ($g = 6$) principal axes of the electron g tensor (Fig. 10, *A* and *B*). EPR (14), x-ray crystallographic (11, 48), and ^{2}H-NMR results[6] all support the idea that the heme residues in the monoclinic type A ($P2_1$) crystals lie approximately in the crystallographic bc^* plane and that the two $g = 6$ components lie in this plane. These conclusions help us predict the type of ESR spectrum to be expected upon sample rotation (about the crystallographic b axis), as shown in Fig. 10.

The effect of sample rotation about an axis in the ab plane is to generate a new powder spectrum with a $g = 2$ component much larger than that seen in the normal powder distribution, Fig. 10, *B* and *C*. This spectrum may be explained as follows. The magnetically ordered crystallites are oriented with their crystallographic c^* axis along the field direction, which coincides with a $g = 6$ g tensor component, at least at low temperatures. The crystallites are, however, disordered with respect to rotation about c^*, in the absence of any other ordering forces (Fig. 5, *E* and *F*). This disorder is not apparent in the ^{2}H-NMR or ESR spectra of the conventionally magnetically ordered samples (Figs. 6*B* and 10*B*) since in the case of deuterium the electric field gradient tensor principal components in different molecules all lie on a conical surface having the same tilt with respect to the H_0 field direction, and in the ESR case c^* seems to correspond closely to a $g = 6$ component at low temperature (Fig. 10*B*), and again all molecules have equivalent relative orientations with respect to the field direction. Rotation of the sample about an axis orthogonal to H_0 in the ^{2}H-NMR case generates a complex tilted conical distribution powder pattern (see for example, Fig. 7*F*). A 90° rotation around any axis in the ab plane generates in the ESR spectrum (Fig. 10*C*) a powder pattern containing all g values between 6 and 2. The resulting powder pattern, therefore, has approximately the width of a normal distribution ($g_x = 5.87$, $g_y = 5.98$, $g_z = 2.00$, Ref. 49) but the lineshape reflects the increased contribution from the $g = 2.00$ component (Fig. 10, *A* and *C*).

This rotation pattern may perhaps be better understood by reference to Fig. 7, *C* and *D*. If we assume that the field (H_0) is along $c^*(y)$, then the vectors in Fig. 7*C* may be visualized as $g = 6$ components. Sample rotation (90°) around $b(x)$ generates a powder spectrum having a large $g = 2$ component. Note that the 90° rotated sample EPR spectrum appears as a powder pattern having g values from 6 to 2 since the original sample has a random distribution of crystallite orientation along c^* (y, see Fig. 5*F*). Thus, on 90° rotation about any axis in the ab plane a powder spectrum having g values from 6 to 2 is obtained (Fig. 10*C*).

Low Spin Ferric Hemes—As discussed above, we have demonstrated the ease with which crystals of the high spin ferric heme-containing protein myoglobin may be ordered by external magnetic fields. Note, however, that the iron atom was in the high spin ferric state. The question now arises as to whether similar effects will be seen with low spin ferric hemoproteins, which we intuitively expect to have small magnetic susceptibilities. Inspection of Equations 11 and 12 suggests for all reasonably sized particles, such as those that may be readily visualized under the light microscope, that such ordering will be observed. This statement of course implies use of a significantly anisotropic g tensor and neglect of the population of excited states, which may be a non-negligible effect for many systems.

Nonetheless, we have found that low spin ferric heme protein microcrystals do indeed orient. We should note at this point that diamagnetic (MbCO) crystals do not orient even at high fields, as evidenced by ^{2}H-NMR at 8.5 Tesla.

We present in Fig. 11 ^{2}H-NMR spectra of the low spin ferric hemoprotein cyanometmyoglobin labeled as C^2H_3 at Met-55 and Met-131. The samples of Fig. 11 were prepared by adding ~20 mg of KCN in saturated $(NH_4)_2SO_4$ to a sample of type A($P2_1$) metaquomyoglobin crystals, followed by pH adjustment and a period of equilibration. The results of Fig. 11*A* were obtained on a solid mass of crystals, obtained by removal of the mother liquor by filtration, although the crystals were still wet and the spectrum obtained is not that characteristic of a dry powder. The spectrum of Fig. 11*A* may be best simulated using a quadrupole splitting ($\Delta\nu_Q$) of 33 kHz and a linewidth (2δ) of 2.8 kHz, Fig. 11*B* and Table I. These simulation parameters are, as expected, very similar to those of the metaquomyoglobin sample (Fig. 6 and Table I).

The sample of Fig. 11*A* when suspended in 90% saturated ammonium sulfate solution and immersed in a magnetic field of 8.5 Tesla orders very rapidly, and the ^{2}H-NMR spectrum of Fig. 11*C* is obtained. Please note, however, that this spectrum is completely different from that obtained for the high spin metaquo complex (Fig. 6). This result is to be expected since the low spin electron g tensor (49) and thus the magnetic susceptibility are expected to be completely different both in

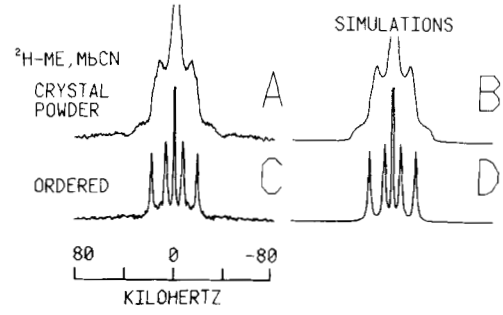

FIG. 11. Deuterium quadrupole echo Fourier transform NMR spectra at 55.3 MHz and 22 ± 1°C of ^{2}H-methylmethionine-labeled sperm whale cyanoferrimyoglobin. *A*, solid powder sample hydrated with 90% saturated $(NH_4)_2SO_4$, 233,644 scans, 65 ms recycle time, $\tau_1 = \tau_2 = 65$ μs, 7 μs 90° pulse widths, 167 kHz spectral width, 4096 real data points, line broadening = 400 Hz. *B*, spectral simulation of the result of *A* using $\Delta\nu_Q = 33.0$ kHz, $\eta = 0.15$, and $2\delta = 2.8$ kHz. *C*, magnetically ordered cyanoferrimyoglobin suspended in ~90% saturated $(NH_4)_2SO_4$, pH = 6.4. 940,703 scans, 61 ms recycle time, $\tau_1 = \tau_2 = 61$ μs, 9 μs 90° pulse widths, 167 kHz spectral width, 4096 real data points, 400 Hz line broadening. *D*, simulation of the spectrum shown in *C* using $\theta_1 = 32.1°$, $\theta_2 = 63.7°$ (or 46.7°), $2\delta = 2.4$ kHz. A small isotropic component was also included in the simulation.

magnitude and orientation to that of the high spin species (49). The crystals, therefore, would appear to orient along a different axis and thus very different ^2H (or ^{13}C) NMR spectra are obtained.

Results obtained using photomicrography of cyanoferrimyoglobin microcrystals (suspended in 90% saturated $(NH_4)_2SO_4$, pH ~6.4) are presented in Fig. 12 and show that, indeed, cyanometmyoglobin crystals orient quite differently to those of metaquomyoglobin. In Fig. 12*A* we show a random distribution of MbCN crystals (×200 on a 5 × 4 inch Polaroid negative) which is essentially identical with that obtained from a random distribution of aquometmyoglobin (Fig. 5*B*). Note in particular the dark crystal (viewed down *a*) and the large capped crystal (viewed down c^*). Upon magnetic ordering all crystals appear capped, and one large well formed crystal and a crystal fragment are shown under high magnification (×400) in Fig. 12*B*. On viewing down *b*, using the technique of sideways ordering followed by a 90° sample rotation for photomicrography, the random distribution of square ended crystals, Fig. 12*C*, is produced. These results show conclusively that MbCN orients approximately along *a* rather than c^*, although it does appear that the crystals have a slight tilt (Fig. 12*b*). The experimental result of Fig. 11*C* thus originates from a sample oriented quite differently to that of metaquomyoglobin. It may be accurately simulated, however, using the parameters listed in Table II, as shown in Fig. 11*D*, in which identical linewidths to those of aquoferrimyoglobin have been used. Quadrupole splittings of $\Delta\nu_Q$ = 13.6 and 38.1 kHz are obtained with MbCN, however, as given in Table II. These quadrupole splittings give solutions for the angles θ' between the electric field gradient tensor principal axis (S^δ—C^ϵ vector) and the field direction of 32.1° (38.1 kHz) and 46.7 or 63.7° (13.6 kHz) at pH 6.4. Two solutions are found for the component nearest the magic angle, since we do not know the sign of $\Delta\nu_Q$, *i.e.* whether the high frequency line is a $0 \leftrightarrow +1$ or $0 \leftrightarrow -1$ transition. The results of Figs. 11 and 12, therefore, indicate that even the low spin ferric heme-containing protein microcrystals may be oriented using the magnetic ordering technique. It, therefore, follows that it should be possible to record ESR spectra of such ordered low spin complexes. This is indeed the case, as shown by the results of Fig. 13.

We show in Fig. 13*A* the 9.3 GHz ESR spectrum of a powder sample of randomly ordered cyanometmyoglobin microcrystals in $(NH_4)_2SO_4$ at very low temperature. The spectrum observed has the shape and width expected on the basis of the work of others (Ref. 49: g_x = 0.93, g_y = 1.89, and g_z = 3.45). A sample ordered at 23° and ~0.7 Tesla for 40 min gives the spectrum of Fig. 13*B*, corresponding to a highly, although not completely, ordered sample, while a sample ordered at 8.5 Tesla for 30 min gives an even sharper spectrum.[5] These results clearly indicate that low spin ferric heme-containing proteins may be oriented even at low magnetic field strengths, consistent with the observation of the very well resolved high field ^2H-NMR spectrum of Fig. 12*C*. Rotation of the sample of Fig. 13*B* by 90° around an axis orthogonal to that of ordering again yields a complex powder distribution with a small g = 3.45 component (Fig. 13*C*).

Particle Size Considerations—The results presented above show that it is a relatively simple matter to obtain high resolution solid state NMR and ESR spectra of protein crystals, which may be used to derive static and in principle dynamic information about protein crystal structure. The time required for a particular sample to order under the influence of the magnetic field may be determined by solution of the appropriate Langevin equation (31). In systems we have studied these times are of the order of minutes, or less, at high magnetic field strengths.

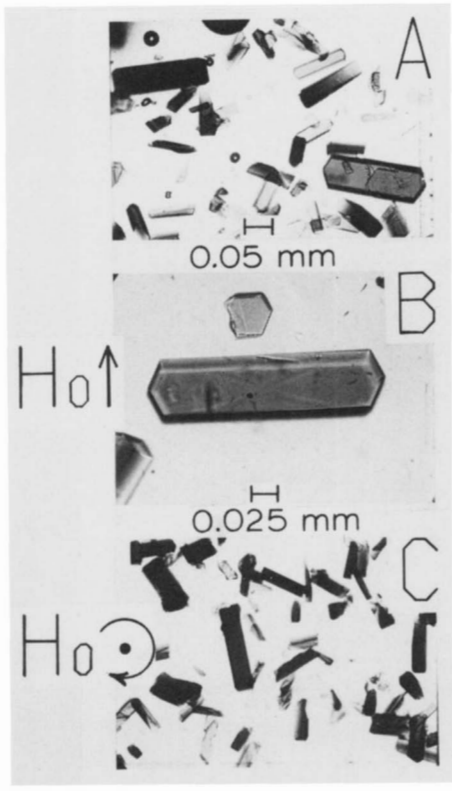

FIG. 12. **Photomicrographs of cyanoferrimyoglobin microcrystals suspended in ~90% saturated $(NH_4)_2SO_4$ at 24 ± 1°C.** *A*, random microcrystalline dispersion, ×200 on a 5 × 4 inch Polaroid negative. *B*, magnetically ordered microcrystals of cyanoferrimyoglobin. The field direction is indicated in the figure, ×400. *C*, "sideways ordered" view of magnetically ordered cyanoferrimyoglobin microcrystalline array, ×200. The axis of ordering is indicated. Note the "pointed" ends of the crystals in *B* and the uniformly square ends of the crystals in the view shown in *C*, where the microcrystals are approximately ordered along the crystallographic *a* axis but disordered about it.

Since we have obtained well ordered samples of low spin ferric heme-containing proteins even at low field (0.3 Tesla) after a few minutes ordering as shown in Fig. 12, it is instructive to estimate the largest dilution of paramagnetic centers possible in a system which might still be ordered due to such centers. Increasing H_0 from 0.3 Tesla to 8.5 Tesla and the g tensor anisotropy term by a factor of at least 3 for a low spin to high spin conversion suggests that for particles of equivalent size to those used in this publication (≳0.1 mm) that species of M_r ~40,000,000 containing one high spin Fe(III) d^5 ion may be highly ordered by a magnetic field of 8.5 Tesla. More dilute samples will still order but more slowly (31). It will of course be realized that this is an exceedingly dilute concentration of paramagnetic centers, and it may well be in some instances that impurities could contribute to the observed effect. Note of course that the binding of these ions must be such that their effects are additive; random binding will not be effective.

In the absence of a magnetic field, it is of some interest to calculate the rate at which the particles will "dephase." For a typical protein having a radius of 20 Å, correlation times of ~1 to 10 ns are expected, from the Stokes-Einstein equation. Using this approximation for crystallites of say 0.1-mm radius leads to correlation times of the order of weeks. In such instances the main causes of disordering will clearly be from mechanical vibrations and possibly by convection. However,

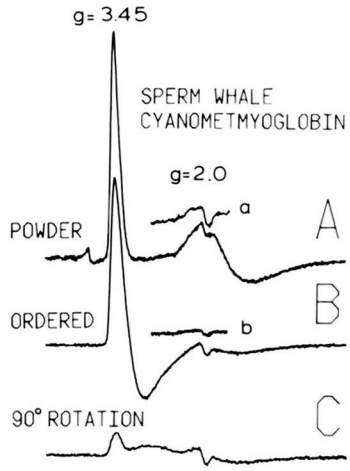

FIG. 13. **9.3 GHz electron spin resonance derivative absorption spectra of sperm whale cyanoferrimyoglobin.** *A*, pH = 6.4, random dispersion in ~90% saturated $(NH_4)_2SO_4$, 4-G modulation amplitude, 7.1°K, 20 milliwatts microwave power. *B*, sample as in *A* but ordered for 40 min at 0.7 Tesla, 1.6-G modulation amplitude, 7°K, 20 milliwatts microwave power. Sample orients considerably more slowly than the high spin derivative and, therefore, the ordering in this spectrum is only partial. *C*, 90° rotation of the sample of *B*, 4-G modulation amplitude, 8°K. *Insets* at *a* and *b* represent the respective cavity contributions.

we have kept samples ordered for several days, which leads to the possibility of preparing ordered systems at very high fields and then carrying out numerous low or zero field (*e.g.* optical) experiments on these materials. Note also that additional ordering may be achieved by the simple expedient of allowing the microcrystals to sediment out under the force of gravity. With metaquomyoglobin for example, a two-dimensional array of crystals may be formed (similar to that shown in Fig. 5*D*) which because of the lack of any need of phase coherence between particles in an NMR experiment should give rise to conventional three-dimensional "rotation patterns."

Experiments with Coboglobins—For high spin ferric hemes there are three Kramers doublets and the zero field splittings D and E are nonzero. If we assume a value $2D \sim 20$ cm^{-1} (50), then it may be seen at room temperature that all three levels will be appreciably populated, since $2D \approx 0.1$ kT. In the absence of generally agreed upon accurate values for D we simply assumed that the contribution to the susceptibility would be dominated by the lower level, irrespective of the g values of the upper levels. This seems to be borne out by experiment since the magnetically ordered ESR spectrum of aquoferrimyoglobin (Fig. 10*B*) shows a very sharp, symmetric absorption at a g value of 6.0 at very low temperature.

A more satisfying check of the magnetic ordering experiment's mechanism is, however, to prepare a protein where the transition metal center is not expected to have additional close-lying Kramer's levels. This is frequently the case for the low spin d^7 ion Co^{II}. We have, therefore, prepared the Co^{II} myoglobin derivative "coboglobin" (51), which has been shown to have inplane g values of $g_{xx} = 2.33$, $g_{yy} = 2.32$, and a g value perpendicular to the plane of the macrocycle of $g_{zz} = 2.09$ (51). The crystals (51) appear isomorphous with those of the ferric heme when grown from 3.2 M $(NH_4)_2SO_4$.

There are many possible ways for the deoxycoboglobin crystals to orient, if they do, in an applied direct current magnetic field. However, we predict that they will orient with $g_{zz} = 2.09$ perpendicular to H_0 (see Equations 10 to 12). We, therefore, expect an "aquomet" (Fig. 5 *C* and *D*) rather than a "cyanomet" (Fig. 12*B*) orientation, since in the latter case g_{max} is approximately perpendicular to the heme plane, and the crystals order approximately along a (Fig. 12*B*).

This prediction is borne out by experiment, as shown in Fig. 14. Fig. 14*A* shows a random distribution of microcrystals of deoxycoboglobin. It can be seen that this distribution is essentially the same as that of metaquomyoglobin (Fig. 5, *A* and *B*). When the sample of Fig. 14*A* is placed in a magnetic field (of 0.3 Tesla strength) an ordered array of microcrystals forms (Fig. 14*B*) which is identical with that obtained with metaquomyoglobin (Fig. 5, *C* and *D*), *i.e.* ordered approximately along c^*, in the heme plane. The orientation of the protein microcrystals showing square (Fig. 5, *C* and *D*; Fig. 14*B*) rather than pointed ends, as found in cyanometmyoglobin (Fig. 12*B*) is that predicted from the orientation of the $g_{\|}$ ~2.09 g tensor components (g_{zz}) determined from the single crystal ESR study of deoxycoboglobin (51), approximately perpendicular to the field direction.

More specifically, we note that ordering along c^* (or c) rather than b may be predicted for both metaquomyoglobin and deoxycoboglobin by examination of the respective g tensors (51, 52). The angles of z, where z is the minimum g value and is along the heme normal, with respect to (a^*, b, c) are (23°, 70°, 79°) for deoxycoboglobin (51) and (22°, 69°, and 73°) for metmyoglobin (52). The minimum energy configuration will clearly be one in which the minimum g value is at 90° to H_0. For both MbH_2O and CoMb this corresponds to H_0 close to c^* (or c), and the crystals should order as observed.

The Resonance Assignments—The correct assignments of the NMR resonances of individual sites in proteins is complex, although many strategies have been developed for assignments in solution NMR spectra (22). In principle, however, assignments in crystal spectra should be simpler than solution assignments if the appropriate crystal structure is known since at least for ^{2}H-NMR it should be possible to predict the NMR spectrum from the crystal structure when the orientation of the crystal in the magnetic field H_0 is known. We have,

FIG. 14. **Photomicrographs of deoxycoboglobin microcrystals suspended in ~90% saturated $(NH_4)_2SO_4$.** *A*, randomly oriented microcrystals, ×200. *B*, microcrystals after ordering for 1 h at 0.3 Tesla, ×200. The axis of ordering is indicated and is apparently very similar to that seen with metaquo(FeIII) myoglobin. The deoxycoboglobin microcrystals order with the $g_{zz} = 2.09$ component perpendicular to the field direction H_0.

therefore, used a combination of x-ray crystallographic data together with the results of spin label broadening experiments to assign the ^{2}H-NMR resonances in Mb to methionine-55 and methionine-131.

Before making any assignments, we first note that the crystal spectra of both MbH_2O and MbCN are pH dependent in the range 6-8. For MbH_2O this is expected since a spin state transition accompanies the formation of Mb·OH (hydroxymetmyoglobin) and Mb·NH_3 (amminemetmyoglobin) in $(NH_4)_2SO_4$ crystals (13). We have shown[5] that this leads to crystal rotation in the magnetic field, so very large spectral changes are predicted. More surprisingly, however, we see significant changes in the spectra of MbCN in the pH range 6.4-7.3, as shown in Fig. 15, which we attribute to small conformational changes in one of the methionine side chains due presumably to titration of a neighboring residue. Please note, however, that there are no appreciable changes observed in carbon-13 NMR solution spectra of methionine residues in myoglobin in this pH range (36) (but not in ammonium sulfate).

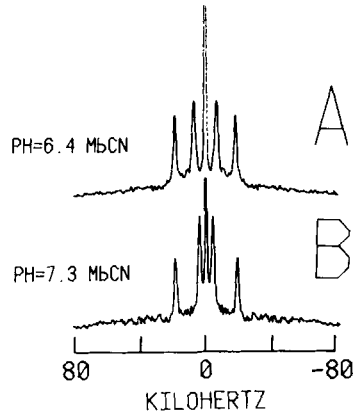

FIG. 15. **Deuterium Fourier transform NMR spectra at 55.3 MHz and 22 ± 1°C of ^{2}H-methylmethionine-labeled cyanoferrimyoglobin from sperm whale (*Physeter catodon*).** *A*, pH = 6.4, sample suspended in ~90% saturated $(NH_4)_2SO_4$. 940,703 scans, recycle time = 61 ms, $\tau_1 = \tau_2 = 61$ μs, 9 μs 90° pulse widths, 167 kHz spectral width, 4096 real data points, 400 Hz line broadening from exponential modification. *B*, sample conditions essentially as in *A* except pH = 7.3 and 201,855 accumulations.

The changes in ^{2}H-NMR spectra seen in the range pH 6.4-7.3 (from $\Delta\nu_Q$ = 13.6 kHz at pH 6.4 to $\Delta\nu_Q$ = 9.3 kHz at pH 7.3) although corresponding to about a 30 to 50% change in quadrupole splitting do occur near the magic angle and in fact correspond to only about a 3° change in the average orientation of the S^δ—C^ϵ vector with respect to the axis of ordering. At pH values intermediate between those indicated, intermediate exchange NMR spectra are obtained, with all the intensity between $\Delta\nu_Q$ = 9.3, 13.6 kHz. This result shows that there is no sign change of $\Delta\nu_Q$ and in addition indicates that the two conformational states have relatively long lifetimes, ≈250 μs at 24°C, pH 6.8.

Addition of a buffered solution of the stable organic free radical 4-amino-2,2,6,6-tetramethyl-piperidinooxyl to microcrystals of MbCN at pH 6.2 (Fig. 16*A*) followed by a ~36-h period of equilibration results in a broadening of the inner resonance. Previous work in solution has strongly suggested that TEMPAMINE only broadens the more exposed Met-55 residue (36); therefore, the 13.6-kHz component of Fig. 16*A* is tentatively assigned to Met-55, and the nonbroadened resonance having $\Delta\nu_Q$ = 38.1 kHz is by elimination tentatively assigned to Met-131. Upon extensive washing, TEMPAMINE is removed and the original ^{2}H-NMR spectrum recovered (Fig. 16*A*). Essentially identical results are obtained with the pH 7.4 MbCN sample (Fig. 16*B*). Note the lack of intensity at a $\Delta\nu_Q$ ~9 kHz in Fig. 16*A* and at ~14 kHz in Fig. 16*B*, supporting the idea that in both cases the pH-dependent conformational change indicated by the results of Fig. 15 does not contribute to the observed line broadenings.

Addition of TEMPAMINE to a sample of MbH_2O at pH ~6.2 results in a broadening of the outer resonance at a $\Delta\nu_Q$ = 53.6 kHz and an unknown effect on the magic angle component having $\Delta\nu_Q$ ~0 kHz (Fig. 16*C*). However, by analogy with the results of Fig. 16, *A* and *B*, we expect only the resonance of the more exposed residue to be broadened due to the presence of the paramagnetic species. The outer component (having $\Delta\nu_Q$ = 53.6 kHz) is, therefore, tentatively assigned to Met-55, and the component under the HO^{2}H signal is assigned to Met-131. Although the second component (under the HO^{2}H signal in Fig. 16*C*) may be resolved in MbF

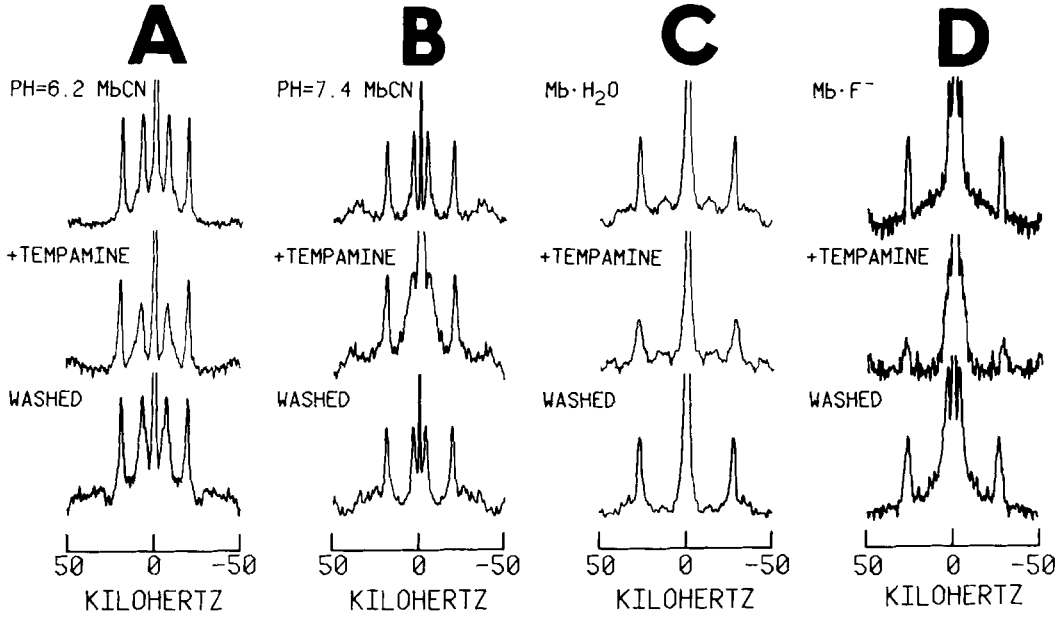

FIG. 16. **Spin label titration of various sperm whale ferrimyoglobins showing selective broadening of one resonance.** *A*, pH 6.2 cyanoferrimyoglobin. *B*, pH 7.4 cyanoferrimyoglobin. *C*, pH 6.2 aquoferrimyoglobin. *D*, pH 7.4 fluoroferrimyoglobin.

(Fig. 16*D*) and in high pH aquometmyoglobin,[5] excessive spectral overlap from the broadened HO^2H resonance and sample stability considerations (high pH sample) have prevented us from accurately monitoring linewidth changes of this resonance upon spin label addition, although it seems clear from the result of Fig. 16*D* that the inner resonance is significantly less effected by addition of TEMPAMINE.

The results of Fig. 16, therefore, give us only very tentative assignments for Met-55 and Met-131. Fortunately, however, since the crystal structure of sperm whale metaquomyoglobin is known (11, 48) these assignments may be compared with those predicted from the x-ray results. A summary of all results is given in Table III.

For MbH_2O, the NMR results give fairly unambiguously values for θ', the angle between the S^δ—C^ϵ bond vector and H_0 (apparently along c^* in MbH_2O, Fig. 5), of $17._5°$ and $54._7°$. Using the crystallographic results (48) we calculate $16._6°$ for Met-55 and $53._4°$ for Met-131, in excellent agreement with the results using the nonpenetrant spin label (Fig. 16*C*). For cyanometmyoglobin, the spin label results at pH 6.2 suggest $\theta = 32._1°$ for Met-131 and $46._7$ or $63._7°$ for Met-55, since the sign of $\Delta\nu_Q$ is not known in the latter instance. Using the crystallographic results for MbH_2O, which are apparently very similar to those for MbCN (53), we obtain closest agreement with the experimental possibilities by assuming that the MbCN crystals order slightly off the a axis, tilted by ~20.5° toward c^*. If this interpretation is correct, then reasonable agreement with the experimental results is obtained (Table III). Since these calculations included use of aquometmyoglobin coordinates (48) perfect agreement should not be expected. The assignments in MbCN are, therefore, more tentative than those for MbH_2O.

TABLE III

Derivation of structural information from quadrupole splitting data and assignment of resonances via spin label titration and from crystallographic coordinates

Data obtained from the spectra of Figs. 6, 11, 15, and 16. Spectra were recorded and samples ordered at 8.5 Tesla (Figs. 6, 11, and 15) or 5.2 Tesla (Fig. 16, spin label titration). The crystallographic coordinates were for sperm whale (*Physeter catodon*) metaquomyoglobin (Ref. 48).

System[a]	Quadrupole splitting	Experimental angle	Theoretical angle
	$\Delta\nu_Q$, kHz[b]	θ', deg[c]	θ', deg
Metaquomyoglobin, pH 6.4	53.6[d]	17.5[d]	16.6[e]
	0.0[f]	54.7[f]	53.4[g]
Cyanometmyoglobin, pH 6.2	13.6[h]	46.7 or 63.7[i]	69.7[j]
	38.1[k]	32.1[k]	25.2[l]
Cyanometmyoglobin, pH 7.4	9.3[h]	49.2 or 60.7[m]	69.7[j]
	39.0[k]	31.5[k]	25.2[l]

[a] Magnetically ordered microcrystals of ~0.1-mm dimensions (see Figs. 5 and 12) suspended in ~90% saturated ammonium sulfate at the pH indicated.

[b] The error is ±500 Hz.

[c] Angle between the principal axis of the electric field gradient tensor (assumed to be colinear with the S^δ—C^ϵ bond vector) and the field direction, H_0. The error varies from ±1° to ±2° and is smallest for angles most removed from the magic angle (54.7°). Quadrupole couplings of 31 kHz (aquometmyoglobin) or 33 kHz (cyanometmyoglobin) were used in the calculations.

[d] Assigned to Met-55 on the basis of spin label titration experiments (Fig. 16*C* and Ref. 36) and calculations from the crystal structure (Ref. 48).

[e] Met-55 (from Ref. 48). The angle is between the S^δ—C^ϵ bond vector and the crystallographic c^* axis.

[f] Assigned to Met-131. See footnote *d* above.

[g] Met-131. See footnote *e* above.

[h] Tentatively assigned to Met-55 on the basis of spin label titration experiment (Fig. 16*A*).

[i] Solution of 63.7 is closest value to x-ray solution using the metaquomyoglobin coordinates (Ref. 48) and with an appropriate crystal tilt. See text for details.

[j] Met-55. Angle is between S^δ—C^ϵ bond vector and the best fit axis of ordering. See the text for details.

[k] Tentatively assigned to Met-131 on the basis of spin label broadening experiment (Fig. 16*A*).

[l] Met-131. See footnote *i* above.

[m] Solution of 60.7° is closest value to x-ray solution. See footnote *i* above.

Other Systems—The results we have presented so far have all been obtained on the rather well characterized small heme protein, myoglobin. Since considerable static and dynamic structural information should be obtained from such high resolution solid state NMR spectra, it is worth considering whether the effect is likely to be a general one or whether it will be applicable solely to small high spin ferric heme-containing proteins. In this context, we have, therefore, investigated another somewhat larger protein, catalase (EC 1.11.1.6). This protein has not yet had its high resolution x-ray diffraction structure reported, due in part to the lack of suitable crystals. Nevertheless, we have obtained highly ordered samples with even the smallest microcrystals, results that suggest that it may be possible to probe catalase and a wide variety of other heme protein structures using NMR and magnetic ordering. Since ordering takes only a few seconds at high field, it may be possible to investigate higher oxidation states (Fe IV) using this method, since freeze trapping of relatively unstable intermediates, followed by high resolution solid state NMR methods should be possible. The technique should also be applicable to determination of substrate-binding geometries, for example by binding ^2H-labeled camphor to cytochrome P-450, and should also be generally applicable to multisubunit proteins, and crystals of differing symmetries. Finally, we note that the technique opens up the possibility of carrying out relaxation studies designed to probe side chain dynamics in protein crystals, which should prove valuable in interpretation of other problems, such as membrane protein dynamics and the problem of protein-lipid interactions.

Acknowledgment—We thank Professors G. N. LaMar and G. Lang for helpful discussions and Mr. Ben Montez for valuable technical assistance. We also thank Dr. R. Jacobs for calculating the tilted conical distribution powder pattern, lineshapes.

REFERENCES

1. Blundell, T. L., and Johnson, L. N. (1976) *Protein Crystallography*, Academic Press, New York
2. Dwek, R. A. (1973) *Nuclear Magnetic Resonance in Biochemistry; Applications to Enzyme Systems*, Clarendon Press, Oxford
3. Wüthrich, K. (1976) *NMR in Biological Research: Peptides and Proteins*, American Elsevier, Inc., New York
4. Gurd, F. R. N., and Rothgeb, T. M. (1979) in *Advances in Protein Chemistry* (Anfinsen, C. B., Edsall, J. T., and Richards, F. M., eds) Vol. 33, p. 73–165, Academic Press, New York
5. Wagner, G., DeMarco, A., and Wüthich, K. (1976) *Biophys. Struct. Mech.* **2,** 139–158
6. Matthews, B. W. (1968) *J. Mol. Biol.* **33,** 491–497
7. Drenth, J., Hol, W. G., Jansonius, J. N., and Koekoek, R. (1971) *Cold Spring Harbor Symp. Quant. Biol.* **36,** 107–116
8. Opella, S. J., Frey, M. H., and Cross, T. A. (1979) *J. Am. Chem. Soc.* **101,** 5856–5857
9. Schaefer, J., and Stejskal, E. O. (1976) *J. Am. Chem. Soc.* **98,** 1031–1032
10. Andrew, E. R. (1971) in *Progress in NMR Spectroscopy* (Emsley, J. W., Feeney, J., and Sutcliffe, L. H., eds) Vol. 8, pp. 1–39, Pergamon Press, New York
11. Kendrew, J. C., and Parrish, R. G. (1956) *Proc. R. Soc. A* **238,** 305–324
12. Norvell, J. C., Nunes, A. C., and Schoenborn, B. P. (1975) *Science* **190,** 568–570
13. Eaton, W. A., and Hochstrasser, R. M. (1968) *J. Chem. Phys.* **49,**

985–995
14. Bennett, J. E., Gibson, J. F., and Ingram, D. J. E. (1957) *Proc. R. Soc. A* **240,** 67–82
15. Chance, B. (1966) in *Hemes and Hemoproteins* (Chance, B., Estabrook, R. W., and Yonetani, T., eds) pp. 213–220, Academic Press, New York
16. Mehring, M. (1976) in *NMR-Basic Principles and Progress* (Diehl, P., Fluck, E., and Kosfeld, R., eds) Vol. 11, pp. 30–39, Springer-Verlag, New York
17. Stark, R. E., Haberkorn, R. A., and Griffin, R. G. (1978) *J. Chem. Phys.* **68,** 1996–1997
18. Oldfield, E., and Rothgeb, T. M. (1980) *J. Am. Chem. Soc.* **102,** 3635–3637
19. Frauenfelder, H., Petsko, G. A., and Tsernoglou, D. (1979) *Nature* **280,** 558–563
20. Artymiuk, P. J., Blake, C. C. F., Grace, D. E. P., Oatley, S. J., Phillips, D. C., and Sternberg, M. J. E. (1979) *Nature* **280,** 563–568
21. Oldfield, E., Norton, R. S., and Allerhand, A. (1975) *J. Biol. Chem.* **250,** 6368–6380
22. Oldfield, E., Norton, R. S., and Allerhand, A. (1975) *J. Biol. Chem.* **250,** 6381–6402
23. Oldfield, E., and Allerhand, A. (1975) *J. Biol. Chem.* **250,** 6403–6407
24. Oldfield, E., and Meadows, M. (1978) *J. Magn. Resonance* **31,** 327–335
25. Slichter, C. P. (1978) *Principles of Magnetic Resonance,* Springer-Verlag, New York
26. Barnes, R. G. (1974) in *Advances in Quadrupolar Research* (Smith, J. A. S., ed) Vol. 1, pp. 335–355, Pergamon Press, New York
27. Oster, O., Neireiter, G. W., Clouse, A. O., and Gurd, F. R. N. (1975) *J. Biol. Chem.* **250,** 7990–7996
28. Wooten, J. B., and Cohen, J. S. (1979) *Biochemistry* **18,** 4188–4191
29. McPherson, A., Jr. (1976) in *Methods of Biochemical Analysis* (Glick, D., ed) Vol. 23, pp. 249–345, Interscience, New York
30. Schlecht, P. (1969) *Biopolymers* **8,** 757–765
31. Trapp, C., Smith, D., and Wasson, J. R. (1969) *J. Chem. Phys.* **51,** 1419–1427
32. Neugebauer, D.-Ch., Blaurock, A. E., and Worcester, D. L. (1977) *FEBS Lett.* **78,** 31–35
33. Brackett, G. C., Richards, P. L., and Caughey, W. S. (1971) *J. Chem. Phys.* **54,** 4383–4401
34. Hapner, K. D., Bradshaw, R. A., Hartzell, C. R., and Gurd, F. R. N. (1968) *J. Biol. Chem.* **243,** 683–689
35. Rothgeb, T. M., and Gurd, F. R. N. (1978) *Methods Enzymol.* **52,** 473–486
36. Jones, W. C., Jr., Rothgeb, T. M., and Gurd, F. R. N. (1976) *J. Biol. Chem.* **251,** 7452–7460
37. Jones, W. C., Jr., Rothgeb, T. M., and Gurd, F. R. N. (1975) *J. Am. Chem. Soc.* **97,** 3875–3877
38. Jaeck, G., and Benz, F. W. (1979) *Biochem. Biophys. Res. Commun.* **86,** 885–892
39. Davis, J. H., Jeffrey, K. R., Bloom, M., Valic, M. I., and Higgs, T. P. (1976) *Chem. Phys. Letts.* **42,** 390–394
40. Oldfield, E., Meadows, M., Rice, D., and Jacobs, R. (1978) *Biochemistry* **17,** 2727–2740
41. Stoll, M. E., Vega, A. J., and Vaughan, R. W. (1977) *Rev. Sci. Instrum.* **48,** 800–803
42. Bloembergen, N., and Rowland, T. J. (1953) *Acta Met* **1,** 731–746
43. Cohen, M. H., and Reif, F. (1957) in *Solid State Physics* (Seitz, F., and Turnbull, D., eds) Vol. 5, pp. 321–438, Academic Press, New York
44. Burnett, L. J., and Muller, B. H. (1971) *J. Chem. Phys.* **55,** 5829–5831
45. Oldfield, E., Gilmore, R., Glaser, M., Gutowsky, H. S., Hsung, J. C., Kang, S. Y., King, T. E., Meadows, M., and Rice, D. (1978) *Proc. Natl. Acad. Sci. U. S. A.* **75,** 4657–4660
46. Campbell, R. F., Meirovitch, E., and Freed, J. (1979) *J. Phys. Chem.* **83,** 525–533
47. Petersen, N. O., and Chan, S. I. (1977) *Biochemistry* **16,** 2657–2667
48. Takano, T. (1977) *J. Mol. Biol.* **110,** 537–568
49. Hori, H. (1971) *Biochim. Biophys. Acta* **251,** 227–235
50. Slade, E. F., and Farrow, R. H. (1972) *Biochim. Biophys. Acta* **278,** 450–458
51. Chien, J. C. W., and Dickinson, L. C. (1972) *Proc. Natl. Acad. Sci. U. S. A.* **69,** 2783–2787
52. Dickinson, L. C., and Chien, J. C. W. (1971) *J. Am. Chem. Soc.* **93,** 5036–5040
53. Watson, H. C., and Chance, B. (1966) in *Hemes and Hemoproteins* (Chance, B., Estabrook, R. W., and Yonetani, T., eds), pp. 149–155, Academic Press, New York